

September 1, 2011

Top-quark production and QCD

NIKOLAOS KIDONAKIS^a AND BEN D. PECJAK^b

^a *Kennesaw State University, Physics #1202
Kennesaw, GA 30144, USA*

^b *Institut für Physik (THEP), Johannes Gutenberg-Universität
D-55099 Mainz, Germany*

Abstract

We review theoretical calculations for top-quark production that include complete next-to-leading-order QCD corrections as well as higher-order soft-gluon corrections from threshold resummation. We discuss in detail the differences between various approaches that have appeared in the literature and review results for top-quark total cross sections and differential distributions at the Tevatron and the LHC.

1 Introduction

Top-quark physics is a centerpiece of the research programs at the Tevatron and the LHC. Due to its unique position as the heaviest particle known to date, the top quark not only plays a role in many models of physics beyond the Standard Model (SM), but also in the precision electroweak fits constraining the mass of the Higgs boson.

The dominant mechanism for creating top quarks at hadron colliders is the production of a top-antitop pair through QCD interactions. Tens of thousands of top-quark pairs have already been produced and studied at the Tevatron since the discovery of the top quark there in 1995 [1, 2], and millions will be produced at the LHC. As the measurements become more precise, it will become increasingly important to have reliable QCD predictions of the total and differential pair-production cross sections. This is true not only if signals of new physics manifest as slight excesses in differential cross sections, but also if top-quark properties are completely determined through the SM. In that case top-quark pair production will be a benchmark process, used in tasks from subtracting backgrounds to constraining gluon PDFs in regions of x relevant for Higgs production.

Another process, with a smaller cross section than for top-antitop, is single top-quark production, which can proceed via three distinct partonic channels. Single top-quark production is important in probing electroweak theory and studying the electroweak properties of the top quark as well as for the discovery of new physics, since the top-quark mass is of the same order of magnitude as the electroweak symmetry breaking scale.

The main purpose of this review is to summarize certain aspects of QCD calculations for the total and differential pair-production cross sections. We will focus on inclusive observables $pp(\bar{p}) \rightarrow t\bar{t}X$, summed over spins, although some results for the single top-quark total cross section in the t -channel, s -channel, and in tW production are also discussed. In particular, we will perform detailed discussions of the total inclusive production cross section, the top-pair invariant mass distribution, the transverse momentum (p_T) distribution of the top (or antitop) quark, and the rapidity distribution, as well as the forward-backward (FB) asymmetry at the Tevatron. While this leaves out a number of interesting topics related to other exclusive observables, these are covered in excellent reviews of top-quark physics in the literature, e.g. [3]. In this review we present in detail the most up-to-date theoretical predictions for the observables mentioned above.

The starting point for a study of inclusive observables in top-quark pair production is the next-to-leading-order (NLO) calculation of differential and total cross sections performed more than two decades ago [4, 5, 6, 7]. However, to keep up with experimental precision requires to go beyond them. Many theorists have responded to this challenge by tackling parts of the diagrammatic calculations needed to reach next-to-next-to-leading-order (NNLO) accuracy and a large number of papers have appeared with pieces of the NNLO calculation. Due to very recent progress it now looks feasible that the NNLO cross section may be available in the near future, a step forward that will mark a major accomplishment.

In the absence of the full NNLO results, an important tool for including higher-order corrections is soft gluon resummation at next-to-leading-logarithm (NLL) accuracy [8, 9] and beyond. The resummation techniques apply to both differential and total cross sections and fixed-order expansions were derived from the NLL resummed cross section with additional

subleading logarithms in [10, 11]. Recently, next-to-next-to-leading-logarithm (NNLL) predictions have appeared for the total cross section [12, 13, 14, 15] and for double differential cross sections with respect to the top quark p_T and rapidity [14, 15, 16], or the pair invariant mass and rapidity [13]. A primary goal of this review is to clarify the similarities and differences between the different approaches.

The remainder of this document is organized as follows. In Section 2 we review the basics of fixed-order calculations to NLO and summarize progress up to NNLO. In Section 3, we discuss the underlying assumptions and techniques in soft gluon resummation, providing a theory comparison of different approaches. We present numerical results for the total inclusive cross section within various approaches in Section 4, for a selected group of differential cross sections in Section 5, and for the FB asymmetry in Section 6. Single top production is briefly discussed in Section 7, and some closing remarks are made in Section 8.

2 Kinematics and fixed-order results

In this section we discuss the basics of fixed-order calculations for inclusive top-quark pair production at hadron colliders. We thus consider the scattering process

$$N_1(P_1) + N_2(P_2) \rightarrow t(p_3) + \bar{t}(p_4) + X, \quad (1)$$

where N_1 and N_2 indicate the incoming protons (LHC) or proton and anti-proton (Tevatron), and X represents an inclusive hadronic final state. The calculation of the differential cross section relies on factorization in QCD. This is the statement that a generic differential hadronic cross section is given in terms of partonic cross sections associated with scattering of gluons and quarks, after a convolution integral with parton distribution functions (PDFs) that describe the parton content of the hadrons. We write this schematically as

$$d\sigma = \sum_{ij \in q, \bar{q}, g} \int dx_1 dx_2 \phi_{i/N_1}(x_1, \mu_F) \phi_{j/N_2}(x_2, \mu_F) d\hat{\sigma}_{ij}(x_1, x_2, \mu_F, \mu_R, \alpha_s(\mu_R)), \quad (2)$$

where the x_i are longitudinal momentum fractions of the incoming partons i , $\phi_{i/N}$ are PDFs, and the $d\hat{\sigma}_{ij}$ are partonic cross sections. The collinear singularities are factorized in a process-independent manner and absorbed into the PDFs, which depend on the factorization scale μ_F . The partonic cross sections can be expanded in a fixed-order series in the strong coupling constant $\alpha_s(\mu_R)$ as

$$d\hat{\sigma}_{ij} = \alpha_s^2 \left[d\hat{\sigma}_{ij}^{(0)} + \frac{\alpha_s}{\pi} d\hat{\sigma}_{ij}^{(1)} + \frac{\alpha_s^2}{\pi^2} d\hat{\sigma}_{ij}^{(2)} \dots \right], \quad (3)$$

where the first term in square brackets is referred to as leading-order (LO), the second term next-to-leading-order (NLO), the third term next-to-next-to-leading-order (NNLO), and so on. The physical cross section is independent of the factorization scale μ_F and the renormalization scale μ_R . However, the truncation of the infinite perturbative series at finite order typically results in a non-negligible numerical dependence.

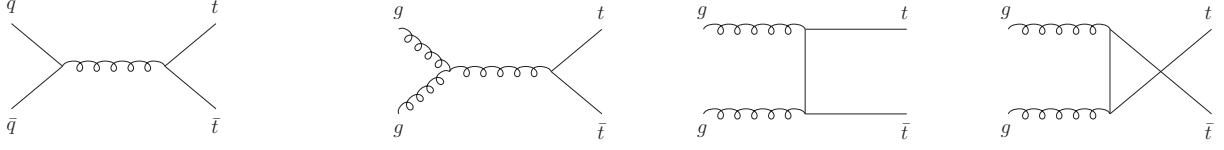


Figure 1: The four Feynman diagrams contributing to top-quark pair production at LO.

At LO, the partonic cross sections receive contributions from the quark-antiquark annihilation and gluon fusion subprocesses

$$\begin{aligned} q(p_1) + \bar{q}(p_2) &\rightarrow t(p_3) + \bar{t}(p_4), \\ g(p_1) + g(p_2) &\rightarrow t(p_3) + \bar{t}(p_4). \end{aligned} \quad (4)$$

The Feynman diagrams needed for the computation of the differential cross section are shown in Figure 1.

The results for the LO differential partonic cross sections read

$$\begin{aligned} \hat{s}^2 \frac{d\hat{\sigma}_{q\bar{q}}^{(0)}}{d\hat{t}_1 d\hat{u}_1} &= \frac{\pi C_F}{N_c} \left(\frac{\hat{t}_1^2 + \hat{u}_1^2}{\hat{s}^2} + \frac{2m_t^2}{\hat{s}} \right) \delta(\hat{s} + \hat{t}_1 + \hat{u}_1), \\ \hat{s}^2 \frac{d\hat{\sigma}_{gg}^{(0)}}{d\hat{t}_1 d\hat{u}_1} &= \frac{2\pi N_c C_F}{(N_c^2 - 1)^2} \left(C_F \frac{\hat{s}^2}{\hat{t}_1 \hat{u}_1} - C_A \right) \left[\frac{\hat{t}_1^2 + \hat{u}_1^2}{\hat{s}^2} + \frac{4m_t^2}{\hat{s}} - \frac{4m_t^4}{\hat{t}_1 \hat{u}_1} \right] \delta(\hat{s} + \hat{t}_1 + \hat{u}_1), \end{aligned} \quad (5)$$

where $C_F = (N_c^2 - 1)/2N_c$ and $C_A = N_c$, with $N_c = 3$ the number of colors in QCD. The partonic Mandelstam variables are defined as

$$\hat{s} = (p_1 + p_2)^2, \quad \hat{t}_1 = (p_1 - p_3)^2 - m_t^2, \quad \hat{u}_1 = (p_2 - p_3)^2 - m_t^2, \quad (6)$$

where m_t is the top quark mass. The partonic momenta are related to the hadronic ones through $p_1 = x_1 P_1$ and $p_2 = x_2 P_2$, so the connection between the hadronic invariants

$$s = (P_1 + P_2)^2, \quad t_1 = (P_1 - p_3)^2 - m_t^2, \quad u_1 = (P_2 - p_3)^2 - m_t^2, \quad (7)$$

and the partonic ones is

$$\hat{s} = x_1 x_2 s, \quad \hat{t}_1 = x_1 t_1, \quad \hat{u}_1 = x_2 u_1. \quad (8)$$

At Born level, any differential cross section can be derived from (5) by an appropriate change of variables. For instance, single-particle-inclusive (1PI) cross sections depending on the rapidity y and p_T of the top quark in the laboratory frame are calculated using

$$t_1 = -\sqrt{s} m_\perp e^{-y}, \quad u_1 = -\sqrt{s} m_\perp e^y, \quad (9)$$

where $m_\perp = \sqrt{p_T^2 + m_t^2}$, while pair-invariant-mass (PIM) observables depending on the pair-invariant mass $M_{t\bar{t}}^2 \equiv (p_3 + p_4)^2$ and scattering angle of the top-quark are obtained using

$$\hat{s} = M_{t\bar{t}}^2, \quad \hat{t}_1 = -\frac{M_{t\bar{t}}^2}{2}(1 - \beta_t \cos \theta), \quad \hat{u}_1 = -\frac{M_{t\bar{t}}^2}{2}(1 + \beta_t \cos \theta). \quad (10)$$

where $\beta_t = \sqrt{1 - 4m_t^2/M_{t\bar{t}}^2}$.

The total cross section itself is conventionally written in the form

$$\sigma(s, m_t) = \frac{\alpha_s^2(\mu_R)}{m_t^2} \sum_{i,j} \int_{4m_t^2}^s \frac{d\hat{s}}{s} \Phi_{ij}\left(\frac{\hat{s}}{s}, \mu_F\right) f_{ij}\left(\frac{4m_t^2}{\hat{s}}, \mu_F, \mu_R\right), \quad (11)$$

where the parton luminosities are defined as

$$\Phi_{ij}(y, \mu_F) = \int_y^1 \frac{dx}{x} \phi_{i/N_1}(x, \mu_F) \phi_{j/N_2}(y/x, \mu_F). \quad (12)$$

The perturbative scaling functions f_{ij} are easily obtained by integrating the differential partonic cross sections over the appropriate phase space. We define their fixed-order expansion as

$$f_{ij} = f_{ij}^{(0)} + 4\pi\alpha_s f_{ij}^{(1)} + (4\pi\alpha_s)^2 f_{ij}^{(2)} + \dots \quad (13)$$

These scaling functions are dimensionless quantities normally written in terms of

$$\beta = \sqrt{1 - \frac{4m_t^2}{\hat{s}}}, \quad \rho \equiv 1 - \beta^2, \quad (14)$$

where at Born level β is just the magnitude of the three-velocity of the top or antitop quark. For reference, the LO expressions in the two channels read

$$\begin{aligned} f_{q\bar{q}}^{(0)} &= \frac{\pi C_F \beta \rho}{12 N_c} [2 + \rho] \\ f_{gg}^{(0)} &= \frac{\pi N_c C_F \beta \rho}{(N_c^2 - 1)^2} \left\{ \frac{1}{\beta} \left[C_F \left(1 + \rho - \frac{\rho^2}{2} \right) + C_A \frac{\rho^2}{4} \right] \ln \left(\frac{1 + \beta}{1 - \beta} \right) - C_F (1 + \rho) - \frac{C_A}{12} (4 + 5\rho) \right\}. \end{aligned} \quad (15)$$

Predictions made using the LO partonic cross sections depend very strongly on the choice of the factorization and renormalization scales and are not appropriate for any sort of detailed phenomenology. However, they are sufficient for understanding most of the qualitative features of the observables discussed later on. For instance, the LO results predict a total cross section of roughly 7 pb at the Tevatron, with a dominant contribution of around 90% from the $q\bar{q}$ channel. At the LHC with $\sqrt{s} = 7$ TeV the cross section is around twenty times as large, and the dominant contribution, of around 75%, is from the gg channel. Obviously, the size of the cross section and relative strength of the different channels reflects the differences in the parton luminosities at the two colliders, since the partonic cross sections are the same.

To make quantitative comparisons between theory and experiment requires the partonic cross sections at NLO accuracy. The total and differential inclusive production cross sections were calculated at NLO more than 20 years ago [4, 5, 6, 7]. All of the NLO results for top-quark pair production are implemented in parton Monte Carlo programs such as MCFM [17] or the NLO version of MadGraph/MadEvent based on [18, 19], or also including parton showers in programs such as MC@NLO [20]. These programs allow for the calculation of

arbitrary differential distributions and are thus an important tool for experimentalists and theorists involved in phenomenological applications.

Numerical results using the partonic cross sections at NLO will be reviewed in the following sections. It is conventional to estimate the theoretical uncertainties associated with the truncation of the perturbative series to NLO by picking default values of the factorization and renormalization scales, varying them up and down by factors of two, and taking the resulting spread of values for the cross section as an indication of the size of uncalculated, higher order terms. Although significantly more stable than LO predictions under such scale variations, NLO calculations still suffer from scale uncertainties of roughly 10-20%. Higher-order calculations using soft-gluon resummation reduce the scale uncertainty and will be covered in the next section. An even more ambitious approach is to calculate the full NNLO corrections, and we now review recent progress in this area.

The calculation of the NNLO cross sections involves two sets of corrections: *i) virtual corrections*, which can be split into genuine two-loop or one-loop squared contributions, and *ii) real radiation*, which involves either one-loop diagrams with the emission of one extra parton in the final state, or tree-level diagrams with two extra partons in the final state. Needless to say, the NNLO calculation is very challenging, and so far only pieces of it are available.

For the virtual corrections, the current situation can be summarized as follows. Analytic results for the two-loop contributions in the high-energy limit are known from [21, 22], along with contributions to the $q\bar{q}$ channel from fermionic [23] and planar corrections [24], and to the gg channel from planar corrections [25]. The exact results for the two-loop contributions in the $q\bar{q}$ channel are known numerically from [26]. In addition, the two-loop infrared singularity structure in the $q\bar{q}$ and gg channels was determined in [27, 28]. Finally, one-loop squared terms were calculated in [29, 30, 31].

For the real corrections, the pieces arising from one-loop virtual-real graphs are known from calculations of $t\bar{t}$ production in association with jets [32, 33, 34, 35]. The more involved task of developing a new subtraction scheme and calculating the contributions from double real radiation has been dealt with in [36, 37, 38, 39, 40]. In light of these advances, the completion of the NNLO calculation now looks feasible, although a significant amount of work is still required to assemble all the elements. In the meantime, approximations of the NNLO corrections are available using techniques from soft gluon resummation.

We end this section with a couple of comments on progress in NLO calculations which is slightly outside the main stream of presentation but nonetheless very important. So far, we have considered only inclusive top-pair production with a final state $t\bar{t}X$. In reality, the top quark decays almost as soon as it is produced, and experiment observes the decay products rather than the top quarks themselves. If the theory calculations stop at the level of on-shell top-quark production, experimentalists must fill in the gaps by correcting their measurements of the decay products (with a possibly complicated set of acceptances) back to that level. Obviously, this should be done as accurately as possible. Recent calculations of top-quark production at NLO, including the top-quark decay in the dominant $t \rightarrow bW$ channel (along with leptonic decay of the W), allow for a much more direct comparison between theory and experiment. The most advanced computations [41, 42] take into account the full correlations between production and decay, without the further assumption of on-shell top-quark production used in the narrow-width approximation. A main result of those works

is that the narrow-width approximation is valid to the percent level for sufficiently inclusive observables (including those studied in this review). This means that in most cases one may use equally well the previous calculations of [43, 44], which include a complete description of production and decay to NLO within the narrow-width approximation.

3 Soft gluon resummation

So far we have considered only the fixed-order perturbative expansion for the partonic cross sections. However, there are certain cases where such an expansion is not the optimal calculational procedure, due the presence of large logarithms related to soft gluon emission. The reorganization of the perturbative expansion in these cases is carried out through techniques referred to as soft gluon resummation.

Soft gluon resummation was first applied to top-quark production at leading-logarithm (LL) accuracy twenty years ago in [45]. At that level the resummation is universal and only depends on the identity of the incoming partons (quarks and gluons) and does not depend on the details of the hard scattering. Other approaches at LL followed in [46, 47] and [48]. However, beyond LL the color structure of the process directly enters the resummation. Resummation for top quark production at NLL was first presented in [8, 9] where the one-loop soft anomalous dimension matrices were calculated. NNLO expansions of the differential resummed cross section, incorporating additional subleading logarithms, were presented in 1PI and PIM kinematics in [10]. A different approach at NLL for the total cross section only, using production threshold, appeared in [49], and was used in [50] and with additional subleading logarithms (and Coulomb terms) in [51].

Further work on two-loop calculations for soft and collinear singularities in massless gauge theories [52, 53, 54, 55, 56, 57] and with massive quarks [58, 59, 60, 61, 62, 27, 28, 13, 63, 64, 14, 15] have eventually allowed NNLL resummation for $t\bar{t}$ production [12, 13, 14, 15, 16].

A typical example where resummation is needed is the top-pair invariant mass distribution at large values of the invariant mass $M_{t\bar{t}}$. To understand why this is the case, consider the factorized expression for the hadronic cross section, which reads

$$\frac{d\sigma}{dM_{t\bar{t}}} = \sum_{i,j} \int_{\tau}^1 \frac{dz}{z} \Phi_{ij}(\tau/z, \mu_F) \frac{d\hat{\sigma}_{ij}(z, M_{t\bar{t}}, \mu_F, \mu_R, \alpha_s(\mu_R))}{dM_{t\bar{t}}}. \quad (17)$$

In the limit of very large invariant mass, the variable $\tau \equiv M_{t\bar{t}}^2/s \rightarrow 1$, which implies that the partonic variable $z \equiv M_{t\bar{t}}^2/\hat{s} \rightarrow 1$. In that limit, the partonic center-of-mass energy is just above the threshold required to produce the top pair with a given invariant mass, which forces any additional radiated partons to be soft. Such soft radiation is associated with IR divergences in the QCD scattering amplitudes, and after collinear subtractions and cancellations with singularities from the virtual corrections, the cross section contains logarithmic plus-distribution corrections. For the n -th order correction to the partonic cross sections in the gg and $q\bar{q}$ channels, these are of the form

$$\alpha_s^n \left[\frac{\ln^m(1-z)}{1-z} \right]_+; \quad m = 0, \dots, 2n-1, \quad (18)$$

where the plus distributions are defined as

$$\int_{\tau}^1 dz \left[\frac{\ln^m(1-z)}{1-z} \right]_+ g(z) = \int_{\tau}^1 dz \frac{\ln^m(1-z)}{1-z} [g(z) - g(1)] + \frac{g(1)}{m+1} \ln^{m+1}(1-\tau) \quad (19)$$

for an arbitrary function $g(z)$. The qg channel also receives up to double logarithmic corrections but it is suppressed by a relative factor of $(1-z)$ compared to the gg and $q\bar{q}$ channels.

The large logarithms appearing in the limit $z \rightarrow 1$ make the perturbative series poorly behaved, and to make reliable predictions requires that they be resummed. Because the logarithms are related to the fact that at the partonic threshold real gluon emission is soft, such a resummation is interchangeably referred to as “soft gluon” or “threshold” resummation. The technical machinery required to perform soft gluon resummation will be reviewed in following two subsections. For now, we just note that the plus-distribution corrections stem from terms depending on the dimensionless ratio $2E_s/\mu$, with $2E_s = \hat{s}(1-z)$ the energy of the soft-gluon radiation in the partonic center-of-mass frame, so the renormalization-group is the basic tool for resummation.

While interesting from the technical point of view, the situation described above is of little phenomenological importance. The reason is that the differential cross section is essentially zero in the limit $\tau \rightarrow 1$, since in that case the combined energy of the top-quark pair approaches the collider energy and the probability that two initial state partons carry such a large fraction of the energy is tiny. Both at the Tevatron and at the LHC, the invariant mass distribution is largest in regions of phase space where τ is closer to zero than to one, and the partonic cross section in the convolution integral (17) is evaluated at values of z far from unity. In that case, the leading terms in the soft limit give the largest contributions to the hadronic cross section if the parton luminosities as a function of τ/z are by far largest at $z \rightarrow 1$. If that is true, then the expansion of the partonic cross section in the $z \rightarrow 1$ limit under the integral (17) is parametrically justified. To a good degree this is an actual property of the parton luminosities, and detailed studies show that, at least at NLO, the leading terms in the $z \rightarrow 1$ limit provide an excellent approximation to the full result. Assuming that also beyond NLO the leading terms in the soft limit account for the bulk of the corrections, then predictions using soft gluon resummation are an improvement on the fixed-order expansion even in regions of phase space where τ is not close to unity.

The line of reasoning used for the invariant mass distribution can be applied to soft gluon resummation for other differential partonic cross sections, or else to the total partonic cross section directly. In fact, the vast literature on soft gluon resummation in top-quark pair production can be broken down into the three main cases shown in Table 1. In each case, one considers the soft limit of the (differential) partonic cross section shown in the table, resums corrections which become large in that limit, and relies on the fall-off of the parton distributions away from the soft limit to dynamically enhance the partonic threshold region. The cases of PIM and 1PI kinematics were first considered in [8, 9] and [65], respectively, and work at the level of double differential cross sections. The logarithmic corrections in PIM kinematics are of the form (19), while in 1PI kinematics they are of form

$$\alpha_s^n \left[\frac{\ln^m(s_4/m_t^2)}{s_4} \right]_+ \quad m = 0, \dots, 2n-1, \quad (20)$$

Name	Observable	Soft limit
pair-invariant-mass (PIM)	$d\sigma/dM_{t\bar{t}}d\theta$	$(1 - z) = 1 - M_{t\bar{t}}^2/\hat{s} \rightarrow 0$
single-particle-inclusive (1PI)	$d\sigma/dp_T dy$	$s_4 = \hat{s} + \hat{t}_1 + \hat{u}_1 \rightarrow 0$
production threshold	σ	$\beta = \sqrt{1 - 4m_t^2/\hat{s}} \rightarrow 0$

Table 1: The three cases in which soft gluon resummation has been applied. The first column indicates the name often used in the literature, the second the observable to which it applies, and the third the partonic variable associated with large logarithmic corrections in the soft limit.

where $s_4 = \hat{s} + \hat{t}_1 + \hat{u}_1$ and the plus distributions are defined as

$$\int_0^{s_4^{\max}} \left[\frac{1}{s_4} \ln^n \left(\frac{s_4}{m_t^2} \right) \right]_+ g(s_4) = \int_0^{s_4^{\max}} ds_4 \frac{1}{s_4} \ln^n \left(\frac{s_4}{m_t^2} \right) [g(s_4) - g(0)] + \frac{g(0)}{n+1} \ln^{n+1} \left(\frac{s_4^{\max}}{m_t^2} \right). \quad (21)$$

It is very important to emphasize that resummed results in 1PI and PIM kinematics are obtained after integrating over a specific portion of the fully differential phase space with respect to additional soft gluon radiation. This means that the results in 1PI or PIM kinematics apply *only* to the differential cross sections in the table, in other words they are not related by a simple change of variables. However, they can both be used to predict the total cross section by integrating over the distributions. Alternatively, one can perform resummation for the total partonic cross section directly working in the production threshold limit, which is the third entry in the table. In that case the large corrections in the soft limit involve simple logarithms of β instead of singular plus distributions.

As far as soft gluon resummation is concerned, results in the production threshold limit are actually a special case of PIM and 1PI kinematics and thus do not contain independent information. For instance, the limit $(1 - z) \rightarrow 0$ plus the additional phase-space restriction $M_{t\bar{t}} \rightarrow 2m_t$, or $s_4 \rightarrow 0$ plus the restriction $\hat{u}_1 + \hat{t}_1 = -4m_t^2$, both imply the limit $\beta \rightarrow 0$. However, in the limit $\beta \rightarrow 0$ there are additional Coulomb singularities of the form $\ln^m \beta/\beta^n$, not all of which are determined by soft gluon resummation alone. In comparing results for the total cross section obtained in the different limits, an important consideration is whether the subleading terms in β contained in the 1PI and PIM results, or the Coulomb singularities are more important. This is a numerical question which we will come back to later on. In the meantime, we pause to explain in more detail the technical formalism needed to perform resummation within the different types of kinematics.

3.1 Mellin-space resummation

The resummation of the threshold logarithms has traditionally been performed in Mellin moment space. By taking moments, divergent distributions in $1 - z$ (PIM kinematics) or s_4 (1PI kinematics) produce powers of $\ln N$, with N the moment variable:

$$\int_0^1 dz z^{N-1} \left[\frac{\ln^m(1-z)}{1-z} \right]_+ = \frac{(-1)^{m+1}}{m+1} \ln^{m+1} N + \mathcal{O}(\ln^{m-1} N). \quad (22)$$

We define moments of the partonic cross section by $\hat{\sigma}(N) = \int dz z^{N-1} \hat{\sigma}(z)$ (PIM) or by $\hat{\sigma}(N) = \int (ds_4/\hat{s}) e^{-Ns_4/\hat{s}} \hat{\sigma}(s_4)$ (1PI). Then the logarithms of N in $\hat{\sigma}(N)$ exponentiate.

Consider the partonic process $f_1 + f_2 \rightarrow t + X$ where X represents the additional final-state particles apart from a produced top quark. We proceed with the derivation of the resummed cross section by writing a factorized form for the moment-space parton-parton scattering cross section, infrared-regularized by ϵ , $\sigma_{f_1 f_2 \rightarrow tX}(N, \epsilon)$, which factorizes as the hadronic cross section

$$\sigma_{f_1 f_2 \rightarrow tX}(N, \epsilon) = \tilde{\phi}_{f_1/f_1}(N, \mu_F, \epsilon) \tilde{\phi}_{f_2/f_2}(N, \mu_F, \epsilon) \hat{\sigma}_{f_1 f_2 \rightarrow tX}(N, \mu_F, \mu_R), \quad (23)$$

where the moments of ϕ are given by $\tilde{\phi}(N) = \int_0^1 dx x^{N-1} \phi(x)$, and for simplicity we do not show the dependence of the cross section on kinematical variables. We factorize the initial-state collinear divergences into the parton distribution functions, ϕ , which are expanded to the same order in α_s as the partonic cross section, and thus obtain the perturbative expansion for the infrared-safe partonic short-distance function $\hat{\sigma}$.

The partonic function $\hat{\sigma}$ is still sensitive to soft-gluon dynamics through its N dependence. We then refactorize the moments of the cross section as [9]

$$\begin{aligned} \sigma_{f_1 f_2 \rightarrow tX}(N, \epsilon) &= \tilde{\psi}_{f_1/f_1}(N, \mu_F, \epsilon) \tilde{\psi}_{f_2/f_2}(N, \mu_F, \epsilon) \\ &\times H_{IL}^{f_1 f_2 \rightarrow tX}(\alpha_s(\mu_R)) \tilde{S}_{LI}^{f_1 f_2 \rightarrow tX}\left(\frac{M}{N\mu_F}, \alpha_s(\mu_R)\right) \prod_j \tilde{J}_j(N, \mu_F, \epsilon) + \mathcal{O}(1/N), \end{aligned} \quad (24)$$

where ψ are center-of-mass distributions that absorb the universal collinear singularities from the incoming partons, H_{IL} is an N -independent function describing the hard-scattering, S_{LI} is a soft gluon function associated with non-collinear soft gluons, and J are functions that absorb the collinear singularities from any massless partons in the final state. We note that the J functions do not appear in the resummation for $t\bar{t}$ production but are needed in single top production via the t - and s -channels.

H and S are matrices in the space of the color structure of the hard scattering, with color indices I and L . The hard-scattering function involves contributions from the amplitude of the process and its complex conjugate, $H_{IL} = h_L^* h_I$.

Using Eqs. (23) and (24) we can write $\hat{\sigma}$ in terms of H , S , J , and the ratios ψ/ϕ . The constraint that the product of these functions must be independent of the gauge and factorization scale results in the exponentiation of logarithms of N in the parton and soft functions [9, 66].

The soft matrix S_{LI} depends on N through the ratio $M/(N\mu_F)$, and it requires renormalization as a composite operator. However, in the product $H_{IL} S_{LI}$ the UV divergences of S are balanced by those of H . S_{LI} satisfies the renormalization group equation [8, 9]

$$\left(\mu \frac{\partial}{\partial \mu} + \beta(g_s) \frac{\partial}{\partial g_s}\right) S_{LI} = -(\Gamma_S^\dagger)_{LB} S_{BI} - S_{LA} (\Gamma_S)_{AI}, \quad (25)$$

where $\beta(g_s)$ is the QCD beta function and $g_s^2 = 4\pi\alpha_s$. Γ_S is the soft anomalous dimension matrix, and it is calculated in the eikonal approximation by explicit renormalization of the soft function. In a minimal subtraction renormalization scheme with $\epsilon = 4 - n$, Γ_S is given at one loop by

$$\Gamma_S^{(1)}(g_s) = -\frac{g_s}{2} \frac{\partial}{\partial g_s} \text{Res}_{\epsilon \rightarrow 0} Z_S(g_s, \epsilon). \quad (26)$$

In processes with simple color structure Γ_S is a 1×1 matrix while in processes with complex color structure it is a non-trivial matrix in color exchange. For quark-antiquark scattering into a top-antitop pair, Γ_S is a 2×2 matrix [8, 9]; for gluon-gluon fusion into a top-antitop pair it is a 3×3 matrix [9].

The exponentiation of logarithms of N in ψ/ϕ and J together with the solution of the renormalization group equation (25), provide us with the complete expression for the resummed partonic cross section in moment space [9]

$$\begin{aligned} \hat{\sigma}^{res}(N) = & \exp \left[\sum_{i=1,2} E^{f_i}(N_i) \right] \exp \left[\sum_j E'^{f_j}(N') \right] \exp \left[\sum_{i=1,2} 2 \int_{\mu_F}^{\sqrt{\hat{s}}} \frac{d\mu}{\mu} \gamma_{i/i}(\tilde{N}_i, \alpha_s(\mu)) \right] \\ & \times \text{Tr} \left\{ H^{f_1 f_2 \rightarrow tX}(\alpha_s(\sqrt{\hat{s}})) \exp \left[\int_{\sqrt{\hat{s}}}^{\sqrt{\hat{s}}/\tilde{N}'} \frac{d\mu}{\mu} \Gamma_S^{\dagger f_1 f_2 \rightarrow tX}(\alpha_s(\mu)) \right] \tilde{S}^{f_1 f_2 \rightarrow tX}(\alpha_s(\sqrt{\hat{s}}/\tilde{N}')) \right. \\ & \left. \times \exp \left[\int_{\sqrt{\hat{s}}}^{\sqrt{\hat{s}}/\tilde{N}'} \frac{d\mu}{\mu} \Gamma_S^{f_1 f_2 \rightarrow tX}(\alpha_s(\mu)) \right] \right\}. \end{aligned} \quad (27)$$

In 1PI kinematics $N_i = N(-\hat{t}_i/M^2)$ for incoming partons i , and $N' = N(\hat{s}/M^2)$; here M is any chosen hard scale relevant to the process, such as the top quark mass. In PIM kinematics $N_i = N' = N$. Also note that $\tilde{N} = N e^{\gamma_E}$, with γ_E the Euler constant.

The first exponent in Eq. (27) arises from the exponentiation of logarithms of N in the ratios ψ/ϕ (the sum $i = 1, 2$ is over incoming partons), and it is given in the $\overline{\text{MS}}$ scheme by

$$E^{f_i}(N_i) = \int_0^1 dz \frac{z^{N_i-1} - 1}{1-z} \left\{ \int_1^{(1-z)^2} \frac{d\lambda}{\lambda} A_i(\alpha_s(\lambda\hat{s})) + D_i[\alpha_s((1-z)^2\hat{s})] \right\}, \quad (28)$$

where A [67, 68] and D [66] have well-known perturbative expansions.

The second exponent in Eq. (27) arises from the exponentiation of logarithms of N in the functions J_j for final-state particles (the sum j is over outgoing quarks and gluons) [67, 68]. It does not appear in $t\bar{t}$ production but is needed for single top quark production.

The third exponent in Eq. (27) controls the factorization scale dependence of the cross section, and $\gamma_{i/i}$ is the moment-space anomalous dimension of the $\overline{\text{MS}}$ density ϕ_{f_i/f_i} . We have $\gamma_{i/i} = -A_i \ln \tilde{N}_i + \gamma_i$ with γ_i the parton anomalous dimensions.

One can evaluate the anomalous dimensions and matching functions appearing in the resummed cross section (27) order-by-order in perturbation theory. The NNLL calculations mentioned at the beginning of the section require the anomalous dimensions A at three loops, all other anomalous dimensions at two loops, and the hard and soft functions at NLO. Obviously, every time a term is added to the anomalous dimensions a whole tower of logarithms in the fixed-order expansion is resummed into the exponent, which accounts for the nomenclature behind this re-organization of the perturbative series. A feature of the resummed cross section in Mellin space is that it contains factors of α_s evaluated below the QCD scale Λ_{QCD} , and is thus subject to Landau-pole ambiguities related to how to deal with this singularity. We will not discuss this issue in detail, but one way of circumventing this problem is to instead construct fixed-order expansions of (27), a topic we return to in Section 3.3.

3.2 Resummation with SCET

We will explain the SCET approach to resummation using PIM kinematics as an illustrative example [13]. The same techniques apply to 1PI kinematics after only small modifications [69]. The starting point is the observation that partonic cross sections near threshold factorize into a product of a hard function, related to virtual corrections, and a soft function, related to real emission in the soft limit [9]. We write this factorization, valid up to corrections of $\mathcal{O}(1-z)$, as¹

$$\frac{d\hat{\sigma}_{ij}(z, M_{t\bar{t}}, m_t, \cos \theta, \mu_F)}{dM_{t\bar{t}} d\cos \theta} = \text{Tr} \left[\mathbf{H}_{ij}(M_{t\bar{t}}, m_t, \cos \theta, \mu_F) \mathbf{S}_{ij}(\sqrt{\hat{s}}(1-z), m_t, \cos \theta, \mu_F) \right]. \quad (29)$$

The boldface indicates that the hard functions \mathbf{H}_{ij} and soft functions \mathbf{S}_{ij} are matrices in color space. In SCET, the separation of the partonic cross sections into a product of hard and soft functions is achieved by a two-step matching procedure from QCD to the effective theory. Hard fluctuations are integrated out in a first step and the hard matching functions are identified as Wilson coefficients of an operator built of soft and collinear fields. Soft fluctuations are integrated out in a second step and the soft matching functions are the Wilson coefficient of a collinear operator, whose matrix element defines the PDFs. Resummation of large logarithms is then performed by deriving and solving the RG equations for the two functions. The main technical complication is that the RG equation for the soft function is non-local. This is dealt with using the Laplace-transform technique introduced in [70], which observed that the Laplace transformed functions

$$\tilde{s}(L, M, m_t, \cos \theta, \mu) = \frac{1}{\sqrt{\hat{s}}} \int_0^\infty d\omega \exp \left(-\frac{\omega}{e^{\gamma_E} \mu e^{L/2}} \right) \mathbf{S}(\omega, M, m_t, \cos \theta, \mu), \quad (30)$$

can be shown to obey local evolution equations whose solution can be inverted back to momentum space analytically.

The final expression for the resummed partonic cross section in PIM kinematics is

$$\begin{aligned} \frac{d\hat{\sigma}(z, M_{t\bar{t}}, m_t, \cos \theta, \mu_F)}{dM_{t\bar{t}} d\cos \theta} &= \exp \left[4a_{\gamma\phi}(\mu_s, \mu_F) - 2a_\Gamma(\mu_s, \mu_F) \ln \frac{M_{t\bar{t}}^2}{\mu_s^2} \right] \\ &\times \text{Tr} \left[\mathbf{U}(M, m_t, \cos \theta, \mu_h, \mu_s) \mathbf{H}(M, m_t, \cos \theta, \mu_h) \mathbf{U}^\dagger(M, m_t, \cos \theta, \mu_h, \mu_s) \right. \\ &\times \left. \tilde{\mathbf{s}}(\partial_\eta, M, m_t, \cos \theta, \mu_s) \right] \frac{e^{-2\gamma_E \eta}}{\Gamma(2\eta)} \frac{1}{(1-z)} \left(\frac{2E_s^{\text{PIM}}(z)}{\mu_s} \right)^{2\eta} \Big|_{\eta=2a_\Gamma(\mu_s, \mu_F)}. \end{aligned} \quad (31)$$

In addition to the hard and soft matching functions, the formula contains factors related to the RG evolution from the matching scales μ_h and μ_s to the factorization scale μ_F . These RG factors are given in terms of integrals over anomalous dimensions; their exact definitions can

¹The parametric scaling $M_{t\bar{t}} \sim m_t$ is assumed, which is valid as long as the top quarks are not too highly boosted.

be found in [13]. For values $\mu_s < \mu_F$ the parameter $\eta < 0$, and one must use a subtraction at $z = 1$ and analytic continuation to express integrals over z in terms of plus distributions. Formula (31) can be evaluated order-by-order in RG-improved perturbation theory, using the standard counting $\ln \mu_h/\mu_s \sim \ln(1-z) \sim 1/\alpha_s$. The current state of the art is NNLL [13], which roughly speaking requires the soft anomalous dimension at two loops (as obtained in [27, 28]) and the hard and soft matching functions to NLO.

Note that the logarithmic corrections at the soft scale are generated by derivatives with respect to η acting on the factors of $(2E_s^{\text{PIM}}(z)/\mu_s)^{2\eta}$. In the SCET calculation, it is natural to use $2E_s^{\text{PIM}}(z) = M_{t\bar{t}}(1-z)/\sqrt{z}$, which is the energy of the soft radiation in the partonic center-of-mass frame. We will refer to such a choice as the PIM_{SCET} scheme. An equally appropriate method, taken in all earlier literature on soft-gluon resummation, is to use the expansion of the energy in the $z \rightarrow 1$ limit, and we will refer to such a choice as the PIM scheme—the situation is summarized in Table 2. The difference between the two schemes involves power-suppressed terms of the form $\ln^n z/(1-z)$ when the formula is re-expanded in fixed order. Such terms appear indeed naturally in the fixed-order calculations, as observed in the case of SCET applications to Drell-Yan [71] and Higgs production [72, 73]. At NLO it can be shown numerically that keeping such terms in the factorized cross section (29) reduces the size of the remaining power-suppressed corrections which vanish in the $z \rightarrow 1$ limit. We will come back to this point in the discussion of approximate NNLO formulas in Section 3.3.

The methods of factorization and resummation described above for the case of PIM kinematics generalizes to that of 1PI kinematics in a straightforward way. In fact, the structure of the resummed formula is exactly as in (31). The main difference is that the expression for the soft function changes, since it is derived by integrating over a different region of the phase space. The hard function, on the other hand, is the same, as is the form of the evolution equations. An analysis to NNLL, which required the calculation of the NLO corrections to the soft function, was performed in [15]. Similarly to the case of PIM kinematics, logarithmic corrections in 1PI kinematics are generated by derivatives acting on a factor of $(2E_s^{1\text{PI}}(s_4)/\mu_s)^{2\eta}$ and one has the choice between identifying this factor with the exact energy of soft-gluon radiation in the \bar{t} rest frame or its expansion in the $s_4 \rightarrow 0$ limit. The two schemes defined in this way are summarized in Table 2. The difference between the 1PI_{SCET} and 1PI schemes involves terms of the form $\ln^n(1+s_4/m_t^2)/s_4$ when expanded in fixed order. Even more so than for the case of PIM kinematics, these subleading terms make an important numerical difference.

The SCET approach to soft-gluon resummation can also be applied to the total cross section in the $\beta \rightarrow 0$ limit. In this limit one can perform soft gluon resummation through the same techniques as in PIM and 1PI kinematics. However, such an approach is insufficient because one must also take into account Coulomb singularities of the form $\ln^m \beta/\beta^n$, and a joint resummation of the two effects is more complicated than soft gluon resummation alone. This issue was solved in [61, 64], which used techniques in SCET and non-relativistic QCD to perform a combined resummation of Coulomb and soft-gluon effects to NNLL order.

From a technical standpoint, resummation within the framework of SCET is very similar to the Mellin-space resummation described in the previous section. In fact, the resummed

PIM _{SCET}	$2E_s^{\text{PIM}}(z) = M_{t\bar{t}}(1-z)/\sqrt{z}$	1PI _{SCET}	$2E_s^{\text{1PI}}(s_4) = s_4/\sqrt{m_t^2 + s_4}$
PIM	$2E_s^{\text{PIM}}(z) = M_{t\bar{t}}(1-z)$	1PI	$2E_s^{\text{1PI}}(s_4) = s_4/m_t$

Table 2: The values of the parameter E_s which define different calculational schemes used in this review.

formulas are completely equivalent if consistently re-expanded to any given order in α_s .² Other than the fact that the SCET results apply directly in momentum space, the main difference between the two approaches is the way in which the soft matching scale μ_s is chosen, and the reasoning underlying this choice. In the SCET approach, one argues that the appearance of a well-separated soft scale at the level of hadronic cross sections is a dynamical effect due to the sharp fall-off of the PDFs away from the partonic threshold region [71]. To determine its numerical value, one studies the corrections arising from the soft function to the differential hadronic cross section as a function of μ_s in fixed order, and finds the value at which these corrections are minimized. This numerical value is a function of the kinematic variables observed in the differential cross section (for instance in PIM kinematics of the invariant mass $M_{t\bar{t}}$), and is interpreted at the scale at which the soft function is free of large logarithmic corrections. Such a choice eliminates the Landau-pole ambiguity, but also implies that the SCET resummation exponentiates a subset of the higher-order plus distributions along with logarithms of the numerical ratio μ_s/μ_F ; a more complete discussion can be found in the Appendix of [15].

3.3 Approximate NNLO formulas

In the previous two sections we focused on all-orders resummation formulas. The basic idea of such formulas is to use properties of real radiation in the soft limit to calculate an infinite set of logarithmic corrections to the partonic cross section in terms of a smaller group of objects such as anomalous dimensions and matching functions. An alternative is to use the same formalism to determine only the logarithmic corrections to a certain accuracy in the fixed-order expansion. This is a useful approximation if it can be argued that such logarithmic terms capture the dominant corrections at a given order, and also that the higher-order logarithmic corrections are not so large as to spoil the convergence of the fixed-order expansion. A benefit of using such an expansion is that the Landau-pole singularities in the Mellin-space formalism are absent, and there is no need to introduce a dynamically generated numerical soft scale in the SCET approach. In this section we explain the structure of approximate NNLO formulas derived from NNLL resummation within the different types of soft limits. We point out that such formulas are subject to a number of ambiguities in the treatment of subleading terms in the soft limit, and discuss how these are dealt with in the literature.

We begin with a discussion of 1PI and PIM kinematics. The approximate NNLO formulas in these cases are applicable to the differential distributions shown in Table 1, but to compare

²This was shown in detail in [70, 74], and later in many other cases, including heavy-quark production in the production threshold limit [61]. The same techniques apply to PIM and 1PI kinematics but an analysis has not yet appeared in the literature.

with the production threshold limit we will work at the level of the total partonic cross section. In PIM kinematics, one can write the general form of the NNLO corrections to the partonic scaling functions (13) as (suppressing the labels for the $q\bar{q}$ and gg channels)

$$f^{(2)}(\beta, \mu) = \int d\cos\theta dz \left[\sum_{n=0}^3 D_n^{\text{PIM}} \left[\frac{\ln^n(1-z)}{1-z} \right]_+ + C^{\text{PIM}} \delta(1-z) + R^{\text{PIM}}(z) \right], \quad (32)$$

while in 1PI kinematics, one can write

$$f^{(2)}(\beta, \mu) = \int d\hat{t}_1 ds_4 \left[\sum_{n=0}^3 D_n^{\text{1PI}} \left[\frac{\ln^n(s_4/m_t^2)}{s_4} \right]_+ + C^{\text{1PI}} \delta(s_4) + R^{\text{1PI}}(s_4) \right]. \quad (33)$$

The D_i , C , and R coefficients are functions of the variables $\hat{s}, \hat{t}_1, \hat{u}_1, m_t, \mu$, so one evaluates the formulas above after an appropriate change of variables. The definition is such that the R coefficients are regular in the limit $z \rightarrow 1$ or $s_4 \rightarrow 0$. Soft gluon resummation at NNLL accuracy determines all of the D_i coefficients in the limit $z \rightarrow 1$ or $s_4 \rightarrow 0$, and also the μ -dependent piece of the delta-function coefficient C [14, 15, 75]. To determine the μ -independent piece of the δ -function coefficient would require the calculation of the soft and hard matching functions at NNLO order. The regular coefficients R are not determined by the soft gluon resummation in the form discussed here and can only be obtained through a complete NNLO calculation.

An alternative to the 1PI and PIM results is to approximate the NNLO corrections through the singular terms in the production threshold limit $\beta \rightarrow 0$. The complete answer was first obtained in [76]. To illustrate its structure, we decompose the NNLO correction to the scaling functions (13) as

$$f_{ij}^{(2)} = f_{ij}^{(2,0)} + f_{ij}^{(2,1)} \ln \left(\frac{\mu_F^2}{m_t^2} \right) + f_{ij}^{(2,2)} \ln^2 \left(\frac{\mu_F^2}{m_t^2} \right). \quad (34)$$

Up to pieces which are regular in the $\beta \rightarrow 0$ limit, the scale-independent corrections read [76]

$$\begin{aligned} f_{q\bar{q}}^{(2,0)} &= \frac{1}{(16\pi^2)^2} \frac{\pi\beta}{9} \left[\frac{3.60774}{\beta^2} + \frac{1}{\beta} \left(-140.368 \ln^2 \beta + 32.106 \ln \beta + 3.95105 \right) \right. \\ &\quad \left. + 910.222 \ln^4 \beta - 1315.53 \ln^3 \beta + 592.292 \ln^2 \beta + 528.557 \ln \beta \right] + \dots, \\ f_{gg}^{(2,0)} &= \frac{1}{(16\pi^2)^2} \frac{7\pi\beta}{192} \left[\frac{68.5471}{\beta^2} + \frac{1}{\beta} \left(496.3 \ln^2 \beta + 321.137 \ln \beta - 8.62261 \right) \right. \\ &\quad \left. + 4608 \ln^4 \beta - 1894.91 \ln^3 \beta - 912.349 \ln^2 \beta + 2456.74 \ln \beta \right] + \dots \end{aligned} \quad (35)$$

Earlier results, which give very similar numerical results for the total cross section although the analytic structure is incorrect, were obtained in [51]. In that paper the coefficients multiplying the μ -dependent logarithms in (34), exact in β , were also presented.

In Section 4 we will compare results for the total top-pair production cross section based on three approximate NNLO calculations available in the literature: the 1PI threshold as implemented in [14], the 1PI and PIM thresholds as implemented in the computer program

from [15], and the production threshold as implemented in the HATHOR program [77]. Since [14] and [15] both use 1PI kinematics and therefore differ only through implementations, it is important to clarify the sources of difference between the 1PI results from [14] and those from the SCET-based approach in [15]. Here there are several issues to consider. First, the numerical results depend on how the relation $\hat{s} + \hat{u}_1 + \hat{t}_1 = 0$ is used in the plus-distribution coefficients (33) before numerical integration, and the two papers in general use different rewritings which are equivalent in the limit $s_4 \rightarrow 0$. Second, even if this relation were used in the same way, there would still be differences in the analytic structure of the approximate NNLO formulas. These definitely affect the μ -dependent part of the δ -function terms, but possibly also the D_0 and μ -independent part of the δ -function terms. The expressions for these coefficients used in [14] can be obtained from [10, 78, 14], while those from [15] were specified in that paper and given in the form of a computer program. Finally, the authors of [15] prefer the 1PI_{SCET} (and PIM_{SCET}) implementation of the approximate NNLO formulas (see Table 2 and the discussion in Section 3.2), where a certain set of subleading terms appearing naturally within the SCET formalism is kept in the regular coefficients R . On the other hand, [14] uses damping factors $2m_t/\sqrt{\hat{s}}$ in the NNLO soft-gluon corrections to the total cross section (for the p_T distributions a damping factor $2m_\perp/\sqrt{\hat{s}}$ is used) in order to reduce the contribution from kinematical regions further away from threshold, and thus improve the 1PI approximation. For the total cross section, the damping factors lead to differences between [14] and [15] that are actually not subleading in the $s_4 \rightarrow 0$ limit of the NNLL calculation. At NLO, the agreement between the exact result for the total cross section and its threshold approximation is improved in both the 1PI_{SCET} scheme and the 1PI scheme with damping factors compared to the pure 1PI expansion. However, at NNLO these different schemes produce rather different results, and the numerical effect of using damping factors versus including subleading SCET terms is greater than that from the other differences in implementation mentioned earlier in this paragraph. More details can be found in the numerical studies in [14] and [15], and also in the comparison in the next section.

4 Total top-pair production cross section

The most basic quantity in top-quark pair production is the total inclusive cross section. In this section we collect numerical results for this quantity based on different levels of perturbative accuracy and discuss the associated uncertainties. We focus on a comparison of NLO and approximate NNLO predictions derived from NNLL resummation in three types of soft limits: production threshold, PIM, and 1PI.

To provide a QCD prediction for the total cross section at a particular collider, one must decide on two things. First, the value of input parameters such as the top-quark mass and a PDF set, and second, a procedure for estimating the theoretical uncertainties associated with the perturbative corrections beyond the accuracy of the calculation. For the NLO calculation, one typically uses scale variations to estimate the uncertainties related to uncalculated corrections at NNLO and beyond. For the approximate NNLO calculations the uncalculated terms include the pieces of the NNLO correction which are subleading in the limit in which the formula is derived. The situation is thus slightly different from a full fixed-order calculation

and there is no conventional way for estimating theoretical uncertainties: some authors use the standard method of scale variations, some use a more complicated procedure. We describe the different approaches in conjunction with the results below.

The results for the cross section in the pole scheme are summarized in Table 3. In addition to the NLO results, we use the following implementation of approximate NNLO predictions:

- Production threshold results as obtained by the HATHOR program [77] with the default settings.
- 1PI results as obtained in [14].
- 1PI_{SCET} and PIM_{SCET} results as obtained in [15]. These are combined into a final result for the cross section using the procedure and computer program presented in [69].

By default, we have set $\mu = \mu_R = \mu_F = m_t$, with $m_t = 173$ GeV. We display NLO results using MSTW2008 NLO PDFs, while for approximate NNLO results we use MSTW2008 NNLO PDFs [79]. Uncertainties in the HATHOR and 1PI results from [14] are estimated by varying μ up and down by a factor of two³, while uncertainties in [69] are estimated by independent variations of μ_R and μ_F by factors of two, along with a scan over the values of the cross section in PIM and 1PI kinematics.

	Tevatron	LHC (7 TeV)
NLO	$6.74^{+0.36+0.37}_{-0.76-0.24}$	160^{+20+8}_{-21-9}
Aliev et. al. [77]	$7.13^{+0.31+0.36}_{-0.39-0.26}$	164^{+3+9}_{-9-9}
Kidonakis [14]	$7.08^{+0.00+0.36}_{-0.24-0.24}$	163^{+7+9}_{-5-9}
Ahrens et. al. [69]	$6.65^{+0.08+0.33}_{-0.41-0.24}$	156^{+8+8}_{-9-9}

Table 3: Results for the total cross section in pb at NLO and within the various NNLO approximations. The first uncertainty is related to perturbative uncertainties, and the second is the PDF error using the MSTW2008 PDF sets [79] at 90% CL.

An examination of the numbers in the table reveals the following features. First, the perturbative uncertainties in the NLO result are on the order of 20% at both the Tevatron and the LHC. This is a bit larger than the PDF uncertainty in both cases, although especially at the LHC one may obtain rather different results with other PDF sets, we refer the reader to [80] for a recent discussion of this issue. Second, the perturbative uncertainties in the approximate NNLO results as obtained through the individual calculations are invariably smaller than at NLO—depending on the implementation, the uncertainties are reduced by a factor of roughly two to three, and are thus under the PDF uncertainties. At the LHC, the different NNLO approximations are in relatively good agreement, though the cross section of [69] is somewhat smaller than in [14, 77]. At the Tevatron, on the other hand, the results from [14, 77] are significantly larger than those from [69]. In fact, the range of values spanned by the three different approximate NNLO results at the Tevatron is about as large as that spanned

³Note that independent variations of μ_F and μ_R in [14] do not increase the uncertainty for LHC energies.

by the NLO calculation. Given the discrepancy, one is faced with the choice of estimating the theory uncertainties through the NLO calculation, with the spread of approximate NNLO values from the three different calculations, or by a particular NNLO approximation alone. The authors of [69, 14, 77] all give arguments in favor of their particular implementation of soft-gluon resummation, but it is beyond the scope of the review to properly summarize them. Instead, we describe very briefly the reasons behind the differences and explain the points which must be addressed to argue for one implementation over the others.

The most important discriminator between the approaches is of course the soft limit in which the resummation is performed. As mentioned before, the production-threshold limit $\beta \rightarrow 0$ is actually a special case of the 1PI and PIM thresholds. At the level of the approximate NNLO formulas, the production threshold results can be obtained from the 1PI and PIM results by re-expanding them in that limit, up to differences related to Coulomb terms (of the form $\ln^m \beta / \beta^n$, see [13] for explicit results) which turn out to be very small numerically [11, 13], particularly at the Tevatron. Therefore, in cases where the production threshold limit differs substantially from the 1PI and PIM cases, it can be concluded that subleading terms in β are not generically small, so arguing for the HATHOR results requires explaining why power corrections to the partonic cross sections do not inherit this generic property and furthermore why the subleading contributions included in the 1PI and PIM results are non-physical. Several differences between the 1PI results of [14] and the SCET-based results of [69] were described in Section 3.3. The numerical importance of various differences is not obvious from the table, since [69] uses a scan over 1PI and PIM kinematics as an estimate of power corrections, but a more detailed study reveals that the dominant effects are the damping factors in [14] or the subleading terms in the 1PI_{SCET} scheme in [69], and less so the differences in the analytic structure described in Section 3.3. Favoring the results of either [14] or [69] thus requires arguments as to why the 1PI results with damping factors or the combination of the SCET implementations of the 1PI and PIM results gives a more reliable estimate of the cross section and its uncertainties.

Recent measurements of the production cross section have been made at the Tevatron CDF [81, 82, 83, 84, 85] and D0 [86, 87, 88, 89, 90, 91] experiments, and the LHC ATLAS [92, 93, 94] and CMS [95, 96, 97] experiments. An especially useful method for comparing with the theory predictions is to show both as a function of the top-quark mass. Then the regions of overlap give a value of the top-quark mass as determined from the production cross section. While the errors in the top-quark mass extracted in this way are larger than those from kinematic distributions in top-quark decay, an advantage is that the theory calculations are carried out in a well-defined renormalization-scheme for the top-quark mass. The results of such analyses carried out through measurements of the lepton + jets channel by the D0 collaboration at the Tevatron appear in [86, 90, 98]. An analogous study has been performed by the ATLAS collaboration at the LHC in [99]. It is also interesting to perform the analysis using short-distance masses such as the $\overline{\text{MS}}$ [12, 69] or threshold masses [69]; results in the $\overline{\text{MS}}$ scheme extracted from Tevatron data can be found in [98]. In Figures 2 and 3 we compare recent experimental measurements assuming a pole mass of $m_t = 172.5$ GeV with the NLO and approximate NNLO predictions, using the same method of estimating perturbative uncertainties as described above and used in Table 3. Although at the Tevatron the central values for an assumed top-quark mass of 172.5 GeV favor the higher values of the cross sec-

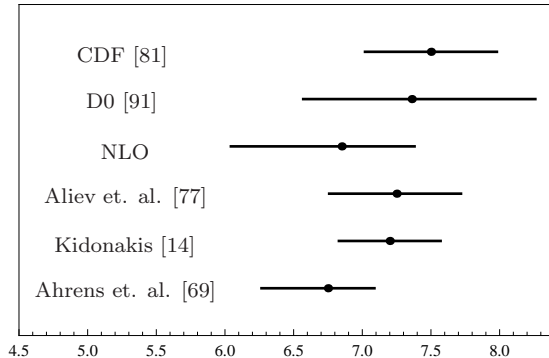


Figure 2: Experimental and theoretical values of the $t\bar{t}$ production cross section in pb at the Tevatron, assuming a top-quark mass of 172.5 GeV. The central values are indicated by the dots, the horizontal lines in the experimental results represent uncertainties from a combination of statistical and systematic errors, and the horizontal lines in the theory results are the perturbative and PDF uncertainties added in quadrature.

tion predicted by [14, 77], the lower values of m_t extracted through the NLO and approximate NNLO calculations from [69] are still within the world average [90].

5 Top quark differential distributions

We now turn to calculations of differential cross sections. To keep in line with the spirit of this review we cover only a few cases: the $t\bar{t}$ invariant mass distribution and the top-quark p_T and rapidity distributions. Results for the pair invariant mass distribution using soft gluon resummation at NLO+NNLL or approximate NNLO exist from the calculations of [13] within PIM kinematics, while those for the p_T and rapidity distributions from the calculations of [14, 15, 16] within 1PI kinematics.

We first discuss the pair invariant-mass distribution. This is an important quantity for phenomenology. It is sensitive to searches for new physics through narrow s -channel resonances, which would show up as bumps in the distribution, while within the SM itself moments of the distribution give additional information about the top-quark mass [101]. Moreover, recent measurements of the forward-backward asymmetry by the CDF collaboration at high values of the pair-invariant mass are much larger than SM predictions, and an important constraint on new physics models which could produce such an excess is the level of agreement of the invariant-mass distribution with the SM calculations. At the Tevatron, this level of agreement is quite good, which we illustrate through the comparison of the CDF result with the NLO+NNLL calculation [13] in Figure 4. Obviously, there are no narrow resonances in the experimental distribution at the Tevatron, and measurements at the LHC will extend this search to higher values of the invariant mass. It is worth emphasizing that at very large values of the invariant mass the theory calculation is more complicated. This is mainly because the top quarks are highly boosted at very high invariant mass, and at some point one must apply an effective theory appropriate for the parametric scaling $m_t \ll M_{t\bar{t}}$. Also, for very

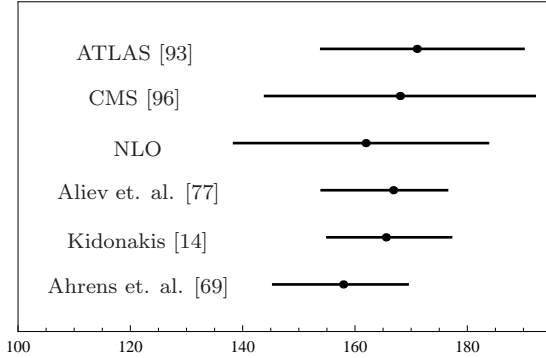


Figure 3: Experimental and theoretical values of the $t\bar{t}$ production cross section in pb at the LHC with $\sqrt{s} = 7$ TeV, assuming a top-quark mass of 172.5 GeV. The central values are indicated by the dots, the horizontal lines in the experimental results represent uncertainties from a combination of statistical and systematic errors, and the horizontal lines in the theory results are the perturbative and PDF uncertainties added in quadrature.

precise predictions, one must account for electroweak corrections, since these contain Sudakov logarithms that grow with the invariant mass [102, 103].

Next, we discuss the top-quark transverse-momentum distribution. Results for the p_T distributions at approximate NNLO at the Tevatron and the LHC with two collider energies are shown in Figure 5, based on the calculations of [14]. These results use MSTW2008 NNLO PDFs with $\mu_F = \mu_R = m_t = 173$ GeV. The D0 collaboration in Ref. [104] has published measurements of the top quark p_T distribution and compared with various theoretical results assuming $m_t = 170$ GeV. We show a comparison of the D0 measurements with the approximate NNLO results from [14] in Figure 6, using scale variation around the central value $\mu_R = \mu_F = m_t = 170$ GeV, and MSTW2008 NNLO PDFs. The agreement between theory [14] and experiment is very good. In Figure 7 we compare the D0 measurements with the NLO and NLO+NNLL calculations from [15]. MSTW2008 PDFs are used, and the theory errors are estimated with scale variations about the default values $\mu_R = \mu_F = 2m_t$, with $m_t = 170$ GeV. The NLO+NNLL predictions from [15] are also in good agreement with the measurements, although the optimal scale-setting procedure for the resummed calculation at higher values of p_T where the distribution is small was left as an open point in that work.

Finally, the NNLO approximate top-quark rapidity distribution at LHC and Tevatron energies from [16] is shown in Fig. 8, using MSTW2008 NNLO PDFs with $\mu_F = \mu_R = m_t = 173$ GeV. The rapidity distribution is important for the top quark forward-backward asymmetry which we discuss in the next section.

Many more plots showing theoretical results for the p_T and rapidity distributions can be found in [14, 15, 16].

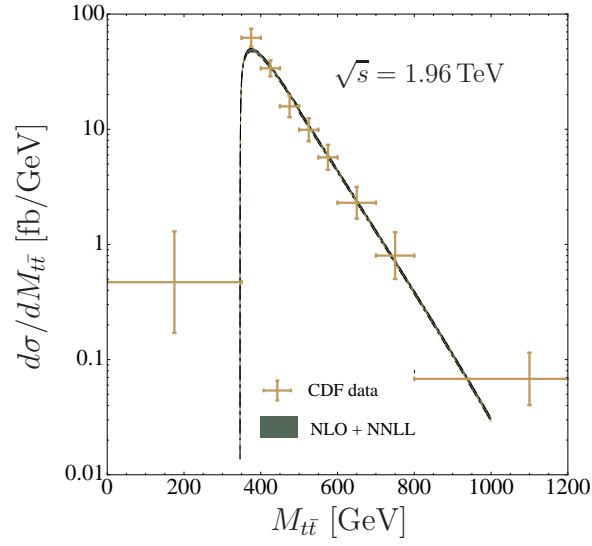


Figure 4: Comparison of NLO+NNLL results [13] for the invariant mass spectrum with CDF measurements [100].

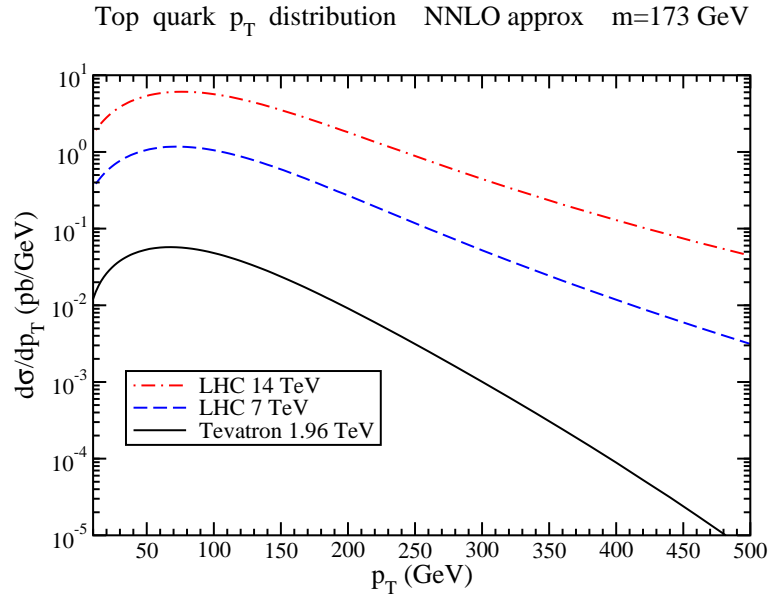


Figure 5: The top quark transverse momentum distribution at the LHC and the Tevatron from [14].

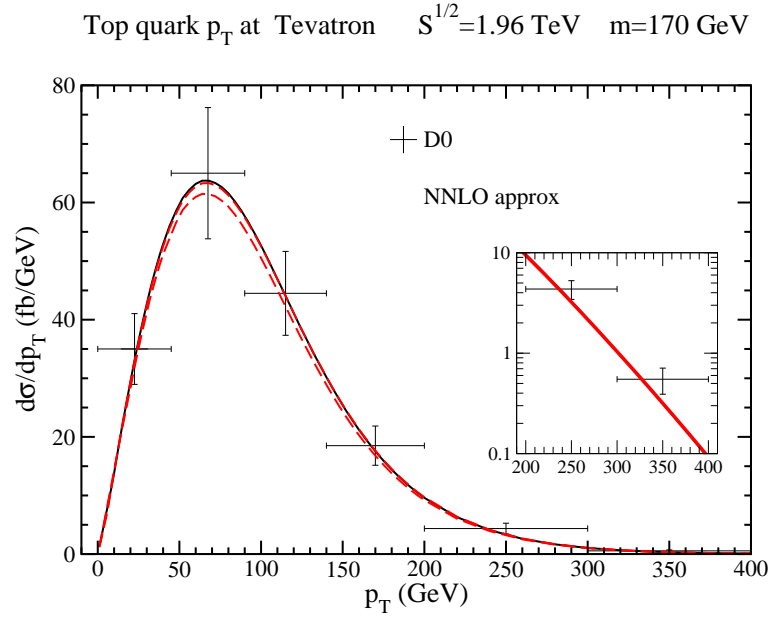


Figure 6: The top quark transverse momentum distribution at the Tevatron from [14] with $m_t = 170$ GeV and $\mu = m_t/2, m_t, 2m_t$ compared with D0 measurements [104].

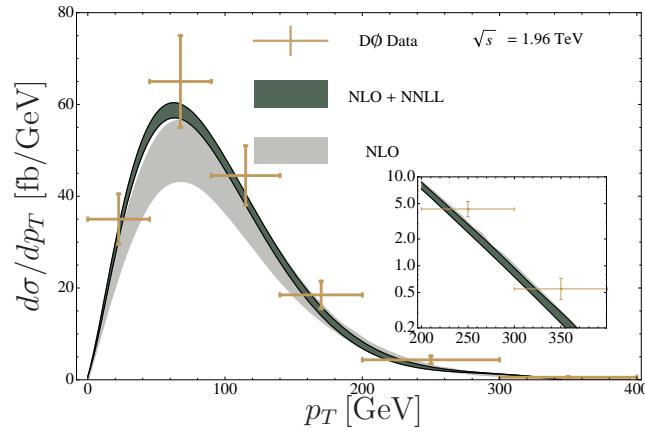


Figure 7: Comparison of NLO+NNLL results [15] for the transverse-momentum distributions with D0 measurements [104].

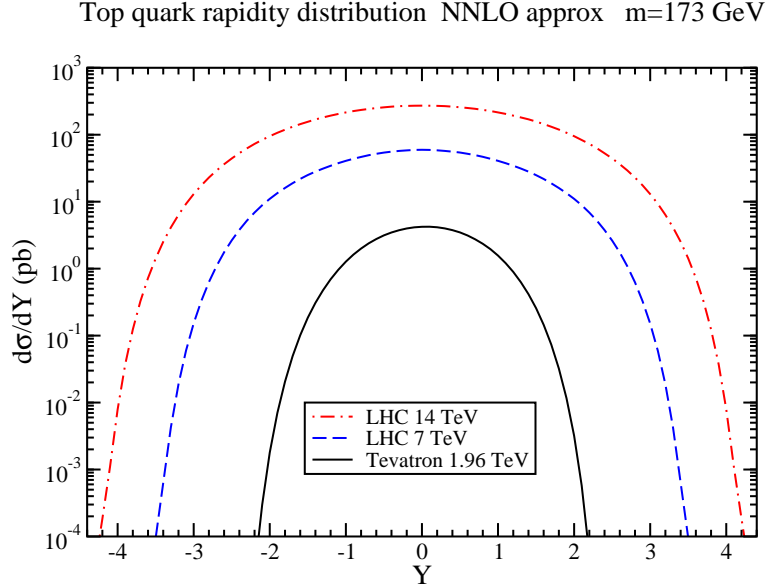


Figure 8: The top quark rapidity distribution at the LHC and the Tevatron from [16].

6 Forward-backward asymmetry

Closely related to differential distributions is the top-pair forward-backward (FB) asymmetry. Its basic definition is

$$A_{\text{FB}}^i = \frac{N(y_t^i > 0) - N(y_t^i < 0)}{N(y_t^i > 0) + N(y_t^i < 0)} = \frac{\sigma(y_t > 0) - \sigma(y_t < 0)}{\sigma(y_t > 0) + \sigma(y_t < 0)} \equiv \frac{\sigma_A^i}{\sigma_S^i}, \quad (36)$$

where N is the number of events and y_t^i is the top-quark rapidity in Lorentz frame i . The definition in terms of the number of events is convenient for experimental measurements, whereas in theory calculations one obtains the forward-backward asymmetric (σ_A) and symmetric (σ_S) cross sections by integrating rapidity distributions over the appropriate values. Since each of these are obtained as a series in α_s , one must further decide whether to re-expand the ratio of asymmetric to symmetric cross sections in the computation of A_{FB} , a point we will come back to in a moment. The basic definition above can also be modified to include cuts on kinematic variables, for instance by imposing that $M_{t\bar{t}}$ or $|y_t|$ is greater or less than a certain value.

At a $p\bar{p}$ collider such as the Tevatron, charge conjugation invariance in QCD implies that $N(y_t^i > 0) = N(y_t^i < 0)$, so the FB asymmetry is equivalent to the charge asymmetry. At a pp collider such as the LHC, rapidity distributions are symmetric and the FB asymmetry vanishes. On the other hand, the production rates for top and antitop quarks at a given rapidity are in general different, so partially integrated charge asymmetries at the LHC do not necessarily vanish. Moreover, one can define non-vanishing total asymmetries with respect to variables such as $|\eta_t| - |\eta_{\bar{t}}|$, with η the pseudorapidity, or $|y_t| - |y_{\bar{t}}|$. Various definitions and results for (partially integrated) charge asymmetries at the LHC can be found elsewhere in this volume [105] and will not be covered here. From now on, we will focus solely on the FB asymmetry at the Tevatron.

Experimental measurements of the FB asymmetry at the Tevatron have been made in the $t\bar{t}$ and $p\bar{p}$ (laboratory) frame.⁴ The measurements of the total asymmetry obtained by the CDF collaboration using 5.3 fb^{-1} of data are [106] $A_{\text{FB}}^{p\bar{p}} = (15.0 \pm 5.5)\%$ ($p\bar{p}$ frame) and $A_{\text{FB}}^{t\bar{t}} = (15.8 \pm 7.5)\%$ ($t\bar{t}$ frame). The quoted uncertainties are derived from a combination of statistical and systematic errors. The measurements are roughly 2σ (1σ) higher than theoretical results in the laboratory ($t\bar{t}$) frame reviewed below. Even more interesting is the measurement as a function of the top-pair invariant mass. After grouping the events in two bins corresponding to $M_{t\bar{t}} \leq 450 \text{ GeV}$ and $M_{t\bar{t}} \geq 450 \text{ GeV}$, the asymmetry in the latter bin was measured to be $A_{\text{FB}}^{t\bar{t}}(M_{t\bar{t}} \geq 450 \text{ GeV}) = (47.5 \pm 11.4)\%$ which is about 3σ higher than the theory predictions in the SM. Attempts to explain the discrepancies of the CDF results with the SM predictions are reviewed in [105]. Here, we present the most up-to-date results for the FB asymmetry within the SM itself, explaining what is known in fixed-order perturbation theory and within different frameworks for soft-gluon resummation.

In the SM the FB asymmetry is due mainly to QCD effects. In fixed-order perturbation theory the asymmetric cross section first appears at $\mathcal{O}(\alpha_s^3)$, in other words at NLO compared to the symmetric cross section. The contributions can be traced to certain types of diagrams in the $q\bar{q}$ channel and qg channels, explicitly identified and calculated in [107, 108]. The gg channel does not contribute to the asymmetric cross section at any order in perturbation theory, because it involves a symmetric initial state. If the ratio σ_A/σ_S in (36) is consistently expanded in α_s , as we will assume to be the case unless otherwise indicated, then the $A_{\text{FB}} \sim \alpha_s$ at the first non-vanishing order. We will label this leading contribution as NLO, with reference to the order at which the differential cross section is needed. The total FB asymmetry at NLO is small in the SM, about 5% in the $p\bar{p}$ frame and 7% in the $t\bar{t}$ frame—exact numbers will be given below. The $q\bar{q}$ channel gives the dominant contribution, while that from the qg channel is much smaller numerically.

Given the potential deviations between the measurements and the SM, it is especially important to estimate the effects of higher-order QCD corrections on the FB asymmetry. This can be done using the methods of soft-gluon resummation. We show results for the total FB asymmetry in the $t\bar{t}$ and $p\bar{p}$ frames at NLO and with soft-gluon resummation included in Table 4. We use MSTW2008 PDFs, with $m_t = 173.1 \text{ GeV}$ for the calculations at NLO+NNLL and $m_t = 173 \text{ GeV}$ at approximate NNLO in the $p\bar{p}$ frame (the numerical difference from the mismatch in the top-quark mass is negligible). The central values refer to the choice $\mu_R = \mu_F = m_t$, and perturbative errors in fixed order are estimated with correlated variations by factors of two; in the resummed result also the matching scales μ_h and μ_s are also varied as described in [109]. In all cases the theory error is much smaller than the experimental one quoted above, and the main qualitative finding is that resummation has only a rather mild effect on the FB asymmetry. This is true whether one uses NLO+NNLL, or the approximate NNLO calculations of [13, 15, 16].⁵ In fact, the same conclusions hold for the invariant-mass dependent CDF analysis, where the asymmetry is studied in a bin below and above a cut at $M_{t\bar{t}} = 450 \text{ GeV}$. The studies in [109] showed that such a binning roughly divides the total

⁴Experiment actually measures the asymmetry with respect to the rapidity difference $y_t - y_{\bar{t}}$, but this is equivalent to (36) in the $t\bar{t}$ frame so we do not distinguish this as a separate observable.

⁵In comparing results it is important to note that [16] does *not* expand the FB asymmetry in α_s , evaluating instead the denominator of (36) numerically at NNLO with no further expansion.

	$A_{\text{FB}}^{t\bar{t}} [\%]$	$A_{\text{FB}}^{p\bar{p}} [\%]$
NLO [109]	$7.32^{+0.69+0.18}_{-0.59-0.19}$	$4.81^{+0.45+0.13}_{-0.39-0.13}$
NLO+NNLL [109]	$7.24^{+1.04+0.20}_{-0.67-0.27}$	$4.88^{+0.20+0.17}_{-0.23-0.18}$
NNLO _{approx.} [16]	—	$5.2^{+0.0}_{-0.6}$

Table 4: The FB asymmetry in the $t\bar{t}$ and $p\bar{p}$ rest frames. The first error refers to perturbative uncertainties estimated through scale variations, the second (where applicable) to PDF uncertainties.

asymmetric cross section in half, and that the effect of resummation in each bin is roughly the same as for the results shown in the table here—in other words, it is a mild effect. Similar conclusions can be drawn from the NLO+NLL study of [110].

The moderate size of the higher-order QCD corrections as estimated by soft gluon resummation makes it important to consider other sources of uncertainty in the SM calculation. First, there are of course subleading terms in the soft limit to which soft-gluon resummation has no access. The magnitude of these terms is estimated through scale variation but will be known for sure only once the fixed-order calculation is done at the next order. Second, electroweak corrections (EW) can also be important for the FB asymmetry. These were considered already in [108], where they were estimated to increase the asymmetry roughly by a factor of 1.1. Refinements related to additional contributions were made in [111], where a slightly smaller contribution was found, but very recently the calculations of [112] quote an increase of about 1.2 due to EW corrections. The corrections for binned analyses in $M_{t\bar{t}}$ and pair rapidity difference were found to be roughly the same in the bins studied by experiment. These corrections are comparable or larger than the QCD uncertainties and thus cannot be ignored—however, they do little to change the 3σ discrepancy between the SM and the CDF measurement in the high invariant-mass bin.

7 Single top production

The observation of single top quark production at the Tevatron [113, 114, 115, 116, 117, 118, 119] and at the LHC [120, 121] has increased the need for reliable theoretical calculations of the cross sections for the corresponding production processes. The single top cross section is less than half of that for $t\bar{t}$ production but the backgrounds are considerable thus making the observation of single tops quite challenging.

Single top quarks can be produced through three distinct partonic processes. One of them is the t -channel process that proceeds via the exchange of a space-like W boson, a second is the s -channel process that proceeds via the exchange of a time-like W boson, and a third is associated tW production. The leading-order diagrams are shown in Fig. 9.

7.1 t -channel production

The t -channel partonic processes are $qb \rightarrow q't$ and $\bar{q}b \rightarrow \bar{q}'t$. At both the LHC and the Tevatron the t -channel is numerically dominant. Calculations of NLO corrections for t -channel

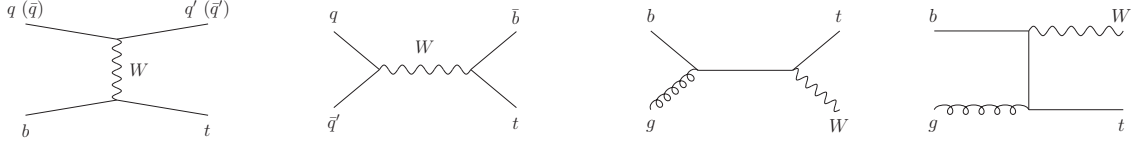


Figure 9: Leading-order t -channel (left), s -channel, and tW (right two) diagrams for single top quark production.

LHC 7 TeV	t	\bar{t}
t -channel [122]	$41.7^{+1.6}_{-0.2} \pm 0.8$	$22.5 \pm 0.5^{+0.7}_{-0.9}$
s -channel [123]	$3.17 \pm 0.06^{+0.13}_{-0.10}$	$1.42 \pm 0.01^{+0.06}_{-0.07}$
tW [124]	$7.8 \pm 0.2^{+0.5}_{-0.6}$	$7.8 \pm 0.2^{+0.5}_{-0.6}$

Table 5: Results for single-top and single-antitop approximate NNLO cross sections at the LHC with $m_t = 173$ GeV in pb. The first uncertainty is from scale variation and the second is the PDF error using the MSTW2008 NNLO PDF sets at 90% CL [79].

production at the differential level have been known for some time [125] (see also further recent NLO studies in [126, 127, 128, 129, 130]).

Theoretical calculations for single top quark production beyond NLO that include higher-order corrections from soft-gluon resummation appeared in [131, 132] at NLL and in [122] at NNLL. The NNLL theoretical expressions in [122] were used to derive approximate NNLO cross sections for t -channel single top or single antitop production at the Tevatron and the LHC.

In Figure 10 the t -channel approximate NNLO cross section from NNLL resummation is plotted versus collider energy, together with recent measurements from the Tevatron [116, 118] and LHC experiments [120, 121]. For a top quark mass of 173 GeV the t -channel single top quark NNLO approximate cross section at the Tevatron is

$$\sigma_{t\text{-ch}}^{\text{top}}(m_t = 173 \text{ GeV}, \sqrt{s} = 1.96 \text{ TeV}) = 1.04^{+0.00}_{-0.02} \pm 0.06 \text{ pb} \quad (37)$$

where the first uncertainty is from scale variation between $m_t/2$ and $2m_t$ and the second is the PDF uncertainty, calculated using the MSTW2008 NNLO PDF sets [79] at 90% C.L. We note that the results for single antitop production at the Tevatron are identical to those for single top.

For t -channel production at the LHC we note that the single top cross section is different from that for single antitop production. For $m_t = 173$ GeV we list the results for LHC 7 TeV energy in Table 5.

7.2 s -channel production

The lowest-order processes in the s -channel are of the form $q\bar{q}' \rightarrow \bar{b}t$, which include the dominant process $u\bar{d} \rightarrow \bar{b}t$ as well as processes involving the charm quark and Cabibbo-

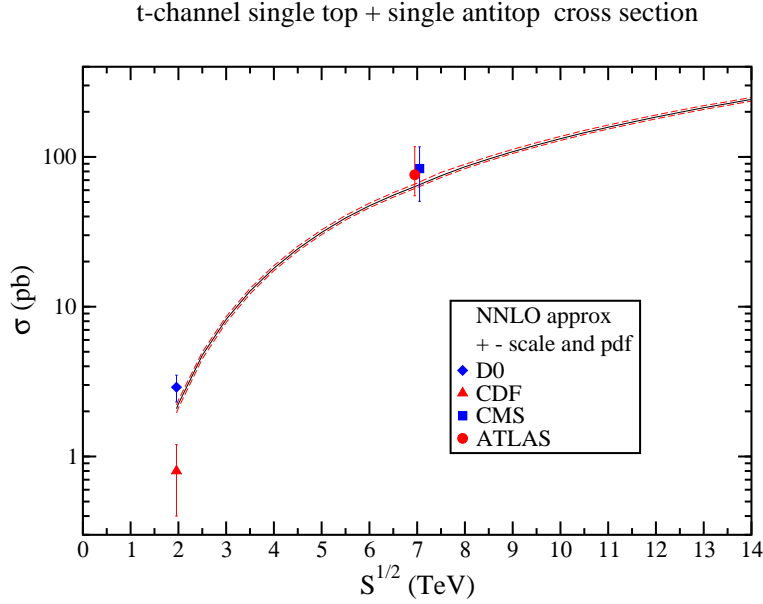


Figure 10: The single top plus single antitop t -channel cross section versus collider energy.

suppressed contributions. The QCD corrections for s -channel production at next-to-leading order (NLO) are known at the differential level [125] and they substantially increase the cross section and stabilize the dependence on the factorization scale.

Approximate NNLO calculations from NLL soft-gluon resummation appeared in [131, 132] and from NNLL resummation in [123]. The soft-gluon corrections dominate the cross section and the NLO expansion of the resummed cross section approximates very well the complete NLO result for both Tevatron and LHC energies. Results based on SCET have appeared in [133]. In addition to the difference in formalism, Refs. [123] and [133] differ in their definitions of the s_4 variable in the resummation; we refer the reader to the papers for a more detailed discussion. Here we just note that contrary to the study in [123] the NLO threshold expansion in the approach of [133] was found to poorly approximate the full corrections at LHC energies.

For a top quark mass of 173 GeV, the s -channel single top cross section and its associated uncertainties at the Tevatron are [123]

$$\sigma_{s\text{-ch}}^{\text{top}}(m_t = 173 \text{ GeV}, \sqrt{s} = 1.96 \text{ TeV}) = 0.523^{+0.001+0.030}_{-0.005-0.028} \text{ pb} \quad (38)$$

where the first uncertainty is from scale variation and the second is the PDF uncertainty at 90% C.L. The results for single antitop production at the Tevatron are identical.

The results for single top and single-antitop s -channel production at the LHC at 7 TeV with $m_t = 173$ GeV are shown in Table 5.

7.3 tW production

The associated production of a top quark with a W boson, $bg \rightarrow tW^-$, is sensitive to new physics and allows a direct measurement of the V_{tb} CKM matrix element. This process is

practically negligible at the Tevatron but it has the second highest cross section among single top processes at the LHC. A similar process in physics beyond the Standard Model is associated production of a top quark with a charged Higgs boson, $bg \rightarrow tH^-$. The next-to-leading order (NLO) corrections to $bg \rightarrow tW^-$ were calculated in [134].

NNLO soft-gluon corrections from NLL resummation were calculated in [131, 132] and from NNLL resummation in [124]. The NLO expansion of the resummed cross section approximates well the complete NLO result for both Tevatron and LHC energies.

The results for tW^- and $\bar{t}W^+$ at the LHC at 7 TeV with $m_t = 173$ GeV are shown in Table 5. The NNLO approximate corrections increase the NLO cross section by $\sim 8\%$. We note that the cross section for $\bar{b}g \rightarrow \bar{t}W^+$ is identical at both Tevatron and LHC to that for $bg \rightarrow tW^-$.

8 Conclusions

We have reviewed QCD calculations for inclusive top-quark production at Tevatron and LHC energies. The total and differential cross sections have been known at NLO in QCD for many years, and more recently different implementations of soft-gluon resummation at NNLL order have also become available and applied to many observables. Compared to NLO calculations, phenomenological predictions based on resummation invariably show smaller dependence on factorization and renormalization scales, and produce moderate changes with respect to central values for a default scale choice. However, especially for the total pair-production cross section at the Tevatron, different forms of resummation can yield results which show only nominal agreement with one another within the quoted uncertainties (see Table 3). We explained in detail the reasons for such differences at the level of approximate NNLO results, but at present the best way of implementing resummation for the total cross section is still subject to debate, as is the most reliable way of estimating the uncertainties. Ultimately, only a complete NNLO calculation will resolve this point.

Acknowledgements

The work of N.K. was supported by the National Science Foundation under Grant No. PHY 0855421.

References

- [1] F. Abe *et al.* [CDF Collaboration], Phys. Rev. Lett. **74**, 2626-2631 (1995). [hep-ex/9503002].
- [2] S. Abachi *et al.* [D0 Collaboration], Phys. Rev. Lett. **74**, 2632-2637 (1995). [hep-ex/9503003].
- [3] W. Bernreuther, J. Phys. G **G35**, 083001 (2008). [arXiv:0805.1333 [hep-ph]].

- [4] P. Nason, S. Dawson, R. K. Ellis, Nucl. Phys. **B303**, 607 (1988).
- [5] P. Nason, S. Dawson, R. K. Ellis, Nucl. Phys. **B327**, 49-92 (1989).
- [6] W. Beenakker, H. Kuijf, W. L. van Neerven, J. Smith, Phys. Rev. **D40**, 54-82 (1989).
- [7] W. Beenakker, W. L. van Neerven, R. Meng, G. A. Schuler, J. Smith, Nucl. Phys. **B351**, 507-560 (1991).
- [8] N. Kidonakis, G. Sterman, Phys. Lett. **B387**, 867 (1996).
- [9] N. Kidonakis, G. Sterman, Nucl. Phys. **B505**, 321 (1997). [hep-ph/9705234].
- [10] N. Kidonakis, R. Vogt, Phys. Rev. **D68**, 114014 (2003). [hep-ph/0308222].
- [11] N. Kidonakis, R. Vogt, Phys. Rev. **D78**, 074005 (2008). [arXiv:0805.3844 [hep-ph]].
- [12] U. Langenfeld, S. Moch, P. Uwer, Phys. Rev. **D80**, 054009 (2009). [arXiv:0906.5273 [hep-ph]].
- [13] V. Ahrens, A. Ferroglia, M. Neubert, B. D. Pecjak, L. L. Yang, JHEP **1009**, 097 (2010). [arXiv:1003.5827 [hep-ph]].
- [14] N. Kidonakis, Phys. Rev. **D82**, 114030 (2010). [arXiv:1009.4935 [hep-ph]].
- [15] V. Ahrens, A. Ferroglia, M. Neubert, B. D. Pecjak, L. L. Yang, [arXiv:1103.0550 [hep-ph]].
- [16] N. Kidonakis, Phys. Rev. **D84**, 011504(R) (2011). [arXiv:1105.5167 [hep-ph]].
- [17] J. M. Campbell, R. K. Ellis, Phys. Rev. **D62**, 114012 (2000). [hep-ph/0006304].
- [18] J. Alwall, P. Demin, S. de Visscher, R. Frederix, M. Herquet, F. Maltoni, T. Plehn, D. L. Rainwater *et al.*, JHEP **0709**, 028 (2007). [arXiv:0706.2334 [hep-ph]].
- [19] R. Frederix, S. Frixione, F. Maltoni, T. Stelzer, JHEP **0910**, 003 (2009). [arXiv:0908.4272 [hep-ph]].
- [20] S. Frixione, P. Nason, B. R. Webber, JHEP **0308** (2003) 007. [hep-ph/0305252].
- [21] M. Czakon, A. Mitov, S. Moch, Phys. Lett. **B651**, 147-159 (2007). [arXiv:0705.1975 [hep-ph]].
- [22] M. Czakon, A. Mitov, S. Moch, Nucl. Phys. **B798**, 210-250 (2008). [arXiv:0707.4139 [hep-ph]].
- [23] R. Bonciani, A. Ferroglia, T. Gehrmann, D. Maitre, C. Studerus, JHEP **0807**, 129 (2008). [arXiv:0806.2301 [hep-ph]].
- [24] R. Bonciani, A. Ferroglia, T. Gehrmann, C. Studerus, JHEP **0908**, 067 (2009). [arXiv:0906.3671 [hep-ph]].

- [25] R. Bonciani, A. Ferroglia, T. Gehrmann, A. Manteuffel, C. Studerus, JHEP **1101**, 102 (2011). [arXiv:1011.6661 [hep-ph]].
- [26] M. Czakon, Phys. Lett. **B664**, 307-314 (2008). [arXiv:0803.1400 [hep-ph]].
- [27] A. Ferroglia, M. Neubert, B. D. Pecjak, L. L. Yang, Phys. Rev. Lett. **103**, 201601 (2009). [arXiv:0907.4791 [hep-ph]].
- [28] A. Ferroglia, M. Neubert, B. D. Pecjak, L. L. Yang, JHEP **0911**, 062 (2009). [arXiv:0908.3676 [hep-ph]].
- [29] J. G. Korner, Z. Merebashvili, M. Rogal, Phys. Rev. **D77**, 094011 (2008). [arXiv:0802.0106 [hep-ph]].
- [30] C. Anastasiou, S. M. Aybat, Phys. Rev. **D78**, 114006 (2008). [arXiv:0809.1355 [hep-ph]].
- [31] B. Kniehl, Z. Merebashvili, J. G. Korner, M. Rogal, Phys. Rev. **D78**, 094013 (2008). [arXiv:0809.3980 [hep-ph]].
- [32] S. Dittmaier, P. Uwer, S. Weinzierl, Phys. Rev. Lett. **98**, 262002 (2007). [hep-ph/0703120 [HEP-PH]].
- [33] S. Dittmaier, P. Uwer, S. Weinzierl, Nucl. Phys. Proc. Suppl. **183**, 196-201 (2008). [arXiv:0807.1223 [hep-ph]].
- [34] G. Bevilacqua, M. Czakon, C. G. Papadopoulos, M. Worek, Phys. Rev. Lett. **104**, 162002 (2010). [arXiv:1002.4009 [hep-ph]].
- [35] K. Melnikov, M. Schulze, Nucl. Phys. **B840**, 129-159 (2010). [arXiv:1004.3284 [hep-ph]].
- [36] M. Czakon, Phys. Lett. **B693**, 259-268 (2010). [arXiv:1005.0274 [hep-ph]].
- [37] M. Czakon, Nucl. Phys. **B849**, 250-295 (2011). [arXiv:1101.0642 [hep-ph]].
- [38] C. Anastasiou, F. Herzog, A. Lazopoulos, JHEP **1103**, 038 (2011). [arXiv:1011.4867 [hep-ph]].
- [39] G. Abelof, A. Gehrmann-De Ridder, JHEP **1104**, 063 (2011). [arXiv:1102.2443 [hep-ph]].
- [40] W. Bernreuther, C. Bogner, O. Dekkers, JHEP **1106**, 032 (2011). [arXiv:1105.0530 [hep-ph]].
- [41] A. Denner, S. Dittmaier, S. Kallweit, S. Pozzorini, Phys. Rev. Lett. **106**, 052001 (2011). [arXiv:1012.3975 [hep-ph]].
- [42] G. Bevilacqua, M. Czakon, A. van Hameren, C. G. Papadopoulos, M. Worek, JHEP **1102**, 083 (2011). [arXiv:1012.4230 [hep-ph]].

- [43] W. Bernreuther, A. Brandenburg, Z. G. Si, P. Uwer, Nucl. Phys. **B690**, 81-137 (2004). [arXiv:hep-ph/0403035 [hep-ph]].
- [44] K. Melnikov, M. Schulze, JHEP **0908**, 049 (2009). [arXiv:0907.3090 [hep-ph]].
- [45] E. Laenen, J. Smith and W. L. van Neerven, Nucl. Phys. B **369**, 543 (1992).
- [46] E. L. Berger and H. Contopanagos, Phys. Lett. B **361**, 115 (1995) [arXiv:hep-ph/9507363].
- [47] E. L. Berger and H. Contopanagos, Phys. Rev. D **54**, 3085 (1996) [arXiv:hep-ph/9603326].
- [48] S. Catani, M. L. Mangano, P. Nason and L. Trentadue, Phys. Lett. B **378**, 329 (1996) [arXiv:hep-ph/9602208].
- [49] R. Bonciani, S. Catani, M. L. Mangano and P. Nason, Nucl. Phys. B **529**, 424 (1998) [Erratum-ibid. B **803**, 234 (2008)] [arXiv:hep-ph/9801375].
- [50] M. Cacciari, S. Frixione, M. L. Mangano, P. Nason, G. Ridolfi, JHEP **0809**, 127 (2008). [arXiv:0804.2800 [hep-ph]].
- [51] S. Moch, P. Uwer, Phys. Rev. **D78**, 034003 (2008). [arXiv:0804.1476 [hep-ph]].
- [52] S. M. Aybat, L. J. Dixon, G. Sterman, Phys. Rev. Lett. **97**, 072001 (2006). [hep-ph/0606254].
- [53] S. M. Aybat, L. J. Dixon, G. Sterman, Phys. Rev. **D74**, 074004 (2006). [hep-ph/0607309].
- [54] L. J. Dixon, L. Magnea, G. Sterman, JHEP **0808**, 022 (2008). [arXiv:0805.3515 [hep-ph]].
- [55] T. Becher, M. Neubert, Phys. Rev. Lett. **102**, 162001 (2009). [arXiv:0901.0722 [hep-ph]].
- [56] T. Becher, M. Neubert, JHEP **0906**, 081 (2009). [arXiv:0903.1126 [hep-ph]].
- [57] E. Gardi, L. Magnea, JHEP **0903**, 079 (2009). [arXiv:0901.1091 [hep-ph]].
- [58] N. Kidonakis, Phys. Rev. Lett. **102**, 232003 (2009). [arXiv:0903.2561 [hep-ph]].
- [59] A. Mitov, G. Sterman, I. Sung, Phys. Rev. **D79**, 094015 (2009). [arXiv:0903.3241 [hep-ph]].
- [60] T. Becher, M. Neubert, Phys. Rev. **D79**, 125004 (2009). [arXiv:0904.1021 [hep-ph]].
- [61] M. Beneke, P. Falgari, C. Schwinn, Nucl. Phys. **B828**, 69-101 (2010). [arXiv:0907.1443 [hep-ph]].

- [62] M. Czakon, A. Mitov, G. Sterman, Phys. Rev. **D80**, 074017 (2009). [arXiv:0907.1790 [hep-ph]].
- [63] A. Mitov, G. Sterman, I. Sung, Phys. Rev. **D82**, 034020 (2010). [arXiv:1005.4646 [hep-ph]].
- [64] M. Beneke, P. Falgari, C. Schwinn, Nucl. Phys. **B842**, 414-474 (2011). [arXiv:1007.5414 [hep-ph]].
- [65] E. Laenen, G. Oderda, G. Sterman, Phys. Lett. **B438**, 173-183 (1998). [hep-ph/9806467].
- [66] H. Contopanagos, E. Laenen, G. Sterman, Nucl. Phys. **B484**, 303-330 (1997). [hep-ph/9604313].
- [67] G. Sterman, Nucl. Phys. **B281**, 310 (1987).
- [68] S. Catani, L. Trentadue, Nucl. Phys. **B327**, 323 (1989).
- [69] V. Ahrens, A. Ferroglia, B. D. Pecjak, L. L. Yang, [arXiv:1105.5824 [hep-ph]].
- [70] T. Becher, M. Neubert, Phys. Rev. Lett. **97**, 082001 (2006). [hep-ph/0605050].
- [71] T. Becher, M. Neubert, G. Xu, JHEP **0807**, 030 (2008). [arXiv:0710.0680 [hep-ph]].
- [72] V. Ahrens, T. Becher, M. Neubert, L. L. Yang, Phys. Rev. **D79**, 033013 (2009). [arXiv:0808.3008 [hep-ph]].
- [73] V. Ahrens, T. Becher, M. Neubert, L. L. Yang, Eur. Phys. J. **C62**, 333-353 (2009). [arXiv:0809.4283 [hep-ph]].
- [74] T. Becher, M. Neubert, B. D. Pecjak, JHEP **0701** (2007) 076. [hep-ph/0607228].
- [75] V. Ahrens, A. Ferroglia, M. Neubert, B. D. Pecjak, L. L. Yang, Phys. Lett. **B687**, 331-337 (2010). [arXiv:0912.3375 [hep-ph]].
- [76] M. Beneke, M. Czakon, P. Falgari, A. Mitov, C. Schwinn, Phys. Lett. **B690**, 483-490 (2010). [arXiv:0911.5166 [hep-ph]].
- [77] M. Aliev, H. Lacker, U. Langenfeld, S. Moch, P. Uwer, M. Wiedermann, Comput. Phys. Commun. **182**, 1034-1046 (2011). [arXiv:1007.1327 [hep-ph]].
- [78] N. Kidonakis, Phys. Rev. **D73**, 034001 (2006). [hep-ph/0509079].
- [79] A. D. Martin, W. J. Stirling, R. S. Thorne, G. Watt, Eur. Phys. J. **C63**, 189-285 (2009). [arXiv:0901.0002 [hep-ph]].
- [80] G. Watt, [arXiv:1106.5788 [hep-ph]].
- [81] CDF Collaboration, Conf. Note 9913.

- [82] T. Aaltonen *et al.* [The CDF Collaboration], Phys. Rev. **D81**, 052011 (2010). [arXiv:1002.0365 [hep-ex]].
- [83] T. Aaltonen *et al.* [The CDF Collaboration], Phys. Rev. **D82**, 052002 (2010). [arXiv:1002.2919 [hep-ex]].
- [84] T. Aaltonen *et al.* [CDF Collaboration], Phys. Rev. **D81**, 092002 (2010). [arXiv:1002.3783 [hep-ex]].
- [85] T. Aaltonen *et al.* [CDF Collaboration], Phys. Rev. **D83**, 071102 (2011). [arXiv:1007.4423 [hep-ex]].
- [86] V. M. Abazov *et al.* [D0 Collaboration], Phys. Rev. Lett. **100**, 192004 (2008). [arXiv:0803.2779 [hep-ex]].
- [87] V. M. Abazov *et al.* [D0 Collaboration], Phys. Rev. **D80**, 071102 (2009). [arXiv:0903.5525 [hep-ex]].
- [88] V. M. Abazov *et al.* [D0 Collaboration], Phys. Rev. **D82**, 032002 (2010). [arXiv:0911.4286 [hep-ex]].
- [89] V. M. Abazov *et al.* [D0 Collaboration], Phys. Rev. **D82**, 071102 (2010). [arXiv:1008.4284 [hep-ex]].
- [90] V. M. Abazov *et al.* [D0 Collaboration], Phys. Rev. **D84**, 012008 (2011). [arXiv:1101.0124 [hep-ex]].
- [91] V. M. Abazov *et al.* [D0 Collaboration], [arXiv:1105.5384 [hep-ex]].
- [92] ATLAS Collaboration, ATLAS-CONF-2011-040.
- [93] ATLAS Collaboration, ATLAS-CONF-2011-100.
- [94] ATLAS Collaboration, ATLAS-CONF-2011-108.
- [95] V. Khachatryan *et al.* [CMS Collaboration], Phys. Lett. **B695**, 424-443 (2011). [arXiv:1010.5994 [hep-ex]].
- [96] S. Chatrchyan *et al.* [CMS Collaboration], JHEP **1107**, 049 (2011). [arXiv:1105.5661 [hep-ex]].
- [97] S. Chatrchyan *et al.* [CMS Collaboration], [arXiv:1106.0902 [hep-ex]].
- [98] V. M. Abazov *et al.* [D0 Collaboration], [arXiv:1104.2887 [hep-ex]].
- [99] ATLAS Collaboration, ATLAS-CONF-2011-054.
- [100] T. Aaltonen *et al.* [CDF Collaboration], Phys. Rev. Lett. **102**, 222003 (2009). [arXiv:0903.2850 [hep-ex]].

- [101] R. Frederix, F. Maltoni, JHEP **0901**, 047 (2009). [arXiv:0712.2355 [hep-ph]].
- [102] W. Bernreuther, M. Fuecker, Z. -G. Si, Phys. Rev. **D74**, 113005 (2006). [hep-ph/0610334].
- [103] J. H. Kuhn, A. Scharf, P. Uwer, Eur. Phys. J. **C51**, 37-53 (2007). [hep-ph/0610335].
- [104] V. M. Abazov *et al.* [D0 Collaboration], Phys. Lett. **B693**, 515-521 (2010). [arXiv:1001.1900 [hep-ex]].
- [105] J. F. Kamenik, J. Shu, J. Zupan, [arXiv:1107.5257 [hep-ph]].
- [106] T. Aaltonen *et al.* [CDF Collaboration], Phys. Rev. **D83**, 112003 (2011). [arXiv:1101.0034 [hep-ex]].
- [107] J. H. Kuhn, G. Rodrigo, Phys. Rev. Lett. **81**, 49-52 (1998). [hep-ph/9802268].
- [108] J. H. Kuhn, G. Rodrigo, Phys. Rev. **D59**, 054017 (1999). [hep-ph/9807420].
- [109] V. Ahrens, A. Ferroglia, M. Neubert, B. D. Pecjak, L. L. Yang, [arXiv:1106.6051 [hep-ph]].
- [110] L. G. Almeida, G. Sterman, W. Vogelsang, Phys. Rev. **D78**, 014008 (2008). [arXiv:0805.1885 [hep-ph]].
- [111] W. Bernreuther, Z. -G. Si, Nucl. Phys. **B837**, 90-121 (2010). [arXiv:1003.3926 [hep-ph]].
- [112] W. Hollik, D. Pagani, [arXiv:1107.2606 [hep-ph]].
- [113] V. M. Abazov *et al.* [D0 Collaboration], Phys. Rev. Lett. **103**, 092001 (2009). [arXiv:0903.0850 [hep-ex]].
- [114] V. M. Abazov *et al.* [D0 Collaboration], Phys. Lett. **B682**, 363-369 (2010). [arXiv:0907.4259 [hep-ex]].
- [115] V. M. Abazov *et al.* [D0 Collaboration], Phys. Lett. **B690**, 5-14 (2010). [arXiv:0912.1066 [hep-ex]].
- [116] V. M. Abazov *et al.* [D0 Collaboration], [arXiv:1105.2788 [hep-ex]].
- [117] T. Aaltonen *et al.* [CDF Collaboration], Phys. Rev. Lett. **103**, 092002 (2009). [arXiv:0903.0885 [hep-ex]].
- [118] T. Aaltonen *et al.* [CDF Collaboration], Phys. Rev. **D82**, 112005 (2010). [arXiv:1004.1181 [hep-ex]].
- [119] T. E. W. Group [CDF and D0 Collaboration], [arXiv:0908.2171 [hep-ex]].
- [120] S. Chatrchyan *et al.* [CMS Collaboration], [arXiv:1106.3052 [hep-ex]].

- [121] ATLAS Collaboration, ATLAS-CONF-2011-088.
- [122] N. Kidonakis, Phys. Rev. **D83**, 091503(R) (2011). [arXiv:1103.2792 [hep-ph]].
- [123] N. Kidonakis, Phys. Rev. **D81**, 054028 (2010). [arXiv:1001.5034 [hep-ph]].
- [124] N. Kidonakis, Phys. Rev. **D82**, 054018 (2010). [arXiv:1005.4451 [hep-ph]].
- [125] B. W. Harris, E. Laenen, L. Phaf, Z. Sullivan, S. Weinzierl, Phys. Rev. **D66**, 054024 (2002). [hep-ph/0207055].
- [126] J. M. Campbell, R. Frederix, F. Maltoni, F. Tramontano, Phys. Rev. Lett. **102**, 182003 (2009). [arXiv:0903.0005 [hep-ph]].
- [127] J. M. Campbell, R. Frederix, F. Maltoni, F. Tramontano, JHEP **0910**, 042 (2009). [arXiv:0907.3933 [hep-ph]].
- [128] P. Falgari, P. Mellor, A. Signer, Phys. Rev. **D82**, 054028 (2010). [arXiv:1007.0893 [hep-ph]].
- [129] R. Schwienhorst, C. -P. Yuan, C. Mueller, Q. -H. Cao, Phys. Rev. **D83**, 034019 (2011). [arXiv:1012.5132 [hep-ph]].
- [130] P. Falgari, F. Giannuzzi, P. Mellor, A. Signer, Phys. Rev. **D83**, 094013 (2011). [arXiv:1102.5267 [hep-ph]].
- [131] N. Kidonakis, Phys. Rev. **D74**, 114012 (2006). [hep-ph/0609287].
- [132] N. Kidonakis, Phys. Rev. **D75**, 071501(R) (2007). [hep-ph/0701080].
- [133] H. X. Zhu, C. S. Li, J. Wang, J. J. Zhang, JHEP **1102**, 099 (2011). [arXiv:1006.0681 [hep-ph]].
- [134] S. Zhu, Phys. Lett. **B524**, 283-288 (2002).